



Universidade de Aveiro Departamento de Física
2008

226000



UNIVERSIDADE DE AVEIRO
SERVIÇOS DE DOCUMENTAÇÃO

Ana Teresa dos Santos Picado **Degradação das marinhas de sal na Ria de Aveiro:
Estudo Hidrodinâmico**

**Degradation of the salt pans in Ria de Aveiro: An
Hydrodynamical Study**

UA-SD



294069



Ana Teresa dos Santos Picado **Degradação das marinhas de sal na Ria de Aveiro:
Estudo Hidrodinâmico**

**Degradation of the salt pans in Ria de Aveiro: An
Hydrodynamical Study**

Dissertação apresentada à Universidade de Aveiro para cumprimento dos requisitos necessários à obtenção do grau de Mestre em Meteorologia e Oceanografia Física, realizada sob a orientação científica do Doutor João Miguel Sequeira Silva Dias, Professor Auxiliar do Departamento de Física da Universidade de Aveiro e co-orientação do Doutor André Bustorff Fortunato Investigador Principal com Habilitação, Núcleo de Estuários e Zonas Costeiras do Laboratório Nacional de Engenharia Civil.

Este trabalho foi desenvolvido no âmbito do projecto MURANO (PTDC/ECM/65589/2006) com o apoio financeiro da Fundação para a Ciência e a Tecnologia - FCT.

o júri

presidente

Prof. Doutor Paulo Manuel Cruz Alves da Silva
Professor Auxiliar do Departamento de Física da Universidade de Aveiro

Prof. Doutor João Miguel Sequeira Silva Dias
Professor Auxiliar do Departamento de Física da Universidade de Aveiro

Doutor André Bustorff Fortunato
Investigador Principal com Habilitação, Núcleo de Estuários e Zonas Costeiras, Laboratório Nacional de Engenharia Civil

Doutor Nuno Alexandre Firmino Vaz
Investigador de Pós-Doutoramento no Instituto Superior Técnico

acknowledgements

It is impossible to carry out a study without the support and active participation of many other people.

To my supervisors, Prof. Doutor João Miguel Dias not only for their scientific supervision but also for the trust, patience, availability and advice at critical moments and Doutor André Fortunato for their availability and advices.

To my friends and colleagues, especially to Magda and Sandra for their support and knowledge and for all the help gave during this year.

To my family that supported me throughout this work in ways less scientific but even more essential.

Thanks Miguel for your support and comprehension.

palavras-chave

Ria de Aveiro, muros das marinhas de sal, modelo hidrodinâmico, prisma de maré, assimetria de maré

resumo

A Ria de Aveiro, uma laguna mesotidal localizada no Noroeste da Costa Portuguesa, é caracterizada por grandes áreas de baixios intermareais e por uma rede de canais estreitos. A laguna apresenta área significativa de marinhas de sal abandonadas, cuja rápida degradação é causada pela falta de manutenção e pelas fortes correntes que provocam a erosão dos seus muros protectores.

O principal objectivo deste trabalho consiste no estudo das consequências na hidrodinâmica de toda a laguna do colapso parcial dos muros das marinhas de sal, através da análise das correntes de maré, do prisma de maré e da assimetria de maré.

Com este objectivo foi implementado e calibrado para a Ria de Aveiro um modelo hidrodinâmico de águas pouco profundas, ELCIRC. A calibração foi realizada ajustando o coeficiente de atrito de fundo, através da comparação entre séries temporais de elevação da superfície livre da água medidas e resultantes do modelo em catorze estações distribuídas ao longo da laguna. Também foi efectuada a análise harmónica comparativa entre estes dados e os resultantes do modelo de modo a avaliar a sua precisão. Uma avaliação dos valores obtidos para os erros médios quadráticos e para o skill mostraram que, apesar de existirem diferenças entre o modelo e os dados, foi conseguida uma boa calibração.

Uma vez calibrado, o modelo ELCIRC foi utilizado para caracterizar a resposta da hidrodinâmica da laguna a alterações batimétricas (aumento da área alagável). Assim, foram geradas diferentes malhas, representando uma inundação sequencial da área central da Ria de Aveiro. Deste modo, várias simulações foram realizadas de forma a avaliar alterações gerais e locais no seu regime hidrodinâmico. A avaliação foi então efectuada através da análise das correntes de maré, do prisma de maré e da assimetria de maré determinadas para caso de estudo.

Os resultados obtidos mostraram que um aumento da área total alagável da laguna, devido ao colapso parcial dos muros das marinhas de sal, resulta num aumento da velocidade da corrente e do prisma de maré, principalmente na área central da laguna e em marés mortas.

A resposta da assimetria de maré, assim como as constantes harmónicas dos constituintes M_2 e M_4 , sofrem também variações em resposta às alterações na área alagável da laguna. Um aumento da área total resulta num decréscimo da amplitude dos constituintes M_2 e M_4 e num aumento da sua fase. Consequentemente, o padrão da assimetria de maré na laguna também é alterado. Em geral, um aumento da área alagável da laguna induz um aumento da assimetria de maré, principalmente no canal de S. Jacinto, no canal do Espinheiro e no início do canal de Ílhavo. Ao longo do canal de Mira o efeito da expansão da área alagada da laguna no padrão de assimetria de maré não é significativo.

keywords

Ria de Aveiro, salt pans walls, hydrodynamic model, tidal currents, tidal prism, tidal asymmetry.

abstract

The Ria de Aveiro, a mesotidal lagoon located on the Northwestern Portuguese coast, is characterized by large areas of intertidal flats and a web of narrow channels. The lagoon has a large area of mostly abandoned salt pans, whose rapid degradation is caused by the lack of maintenance and by the strong currents which erode their protector walls.

The main aim of this work was to study the consequence of the salt pans walls partial collapse on the entire lagoon hydrodynamics, through the analysis of tidal currents, tidal prism and tidal asymmetry.

With this purpose a shallow water model, ELCIRC, was implemented and calibrated for the Ria de Aveiro. The calibration was performed by adjusting the bottom friction coefficients, through the comparison between measured and computed time series of surface water elevations at fourteen stations distributed within the lagoon. Comparative harmonic analyses of those data and of the model results were also performed in order to evaluate the models accuracy. An assessment of the root mean square errors and skill showed that a good calibration was achieved, although differences between model and field data exist.

Once calibrated, ELCIRC was used to characterize the response of the lagoon hydrodynamics to bathymetric changes (increase of the flooded area). Thus, distinct grids were generated representing a sequential flooding of the Ria de Aveiro central area. Several simulations were performed in order to evaluate possible changes in overall and local lagoon's hydrodynamic regime. This evaluation was performed through the analysis of tidal currents, tidal prism and tidal asymmetry for each case study.

The results show that an increase of the lagoon total flooded area, due to the salt pans walls partial collapse, produces an increase of the tidal currents magnitude and the tidal prism, mainly in the lagoon central area and with largest changes in neap tide condition.

The responses of tidal asymmetry, as well as the harmonic constants of M_2 and M_4 constituents, were also affected by changes in the lagoon total flooded area. An increase in the total area of the lagoon results in a decrease of M_2 and M_4 amplitudes and in an increase of their phases. Thereby, the tidal asymmetry pattern in the lagoon is also changed. In general, an increase in the lagoon flooded area leads to an increase in the tidal asymmetry, mainly along the S. Jacinto, Espinheiro and at the beginning of Ílhavo channels. Along the Mira channel the effect of the expansion of the lagoon flooded in tidal asymmetry pattern is not significant.

Contents

Acknowledgements	i
Resumo	iii
Abstract	v
List of Figures	ix
List of Tabela	xi
1. Introduction	1
1.1. Motivation and Aims	1
1.2. Structure of this work	2
1.3. State of the Art	2
2. The Study Area	5
2.1 Description of the study area	5
2.2 Field Data	7
3. Numerical model	11
3.1. Model Description	11
3.2. Model Establishment	12
3.3. Hydrodynamic Model Calibration	14
4. Hydrodynamic changes induced by salt pans walls degradation	27
4.1 Tidal Currents	28
4.2 Tidal Asymmetry	32
4.3 Tidal Prism	37
5. Conclusion	41
6. References	45

List of Figures

2.1:	Ria de Aveiro lagoon.	5
2.2:	Salt pans of Ria de Aveiro lagoon.	7
2.3:	Ria de Aveiro bathymetry, represented in UTM coordinates, with depth in meters relative to the hydrographic null (-2.00 m below mean sea level) and with locations of the stations where field data is available.	9
3.1:	Horizontal grid of Ria de Aveiro: a) Old grid; b) New grid.	13
3.2:	Detail of the grid near the study area: a) Old grid; b) New grid.	13
3.3:	Ria de Aveiro lagoon numerical bathymetry, with depth in meters relative to the mean sea level (2 m) and with the locations of the stations used in the calibration of the numeric model: a) Entire lagoon; Detail of bathymetry near the inlet b) and near the study area c).	14
3.4:	Comparison between predicted and observed sea surface elevation (solid line: model results; circles: measurements). In the panels are referred the beginning and the end of each compared period.	16
3.5:	Comparison between predicted and observed sea surface elevation (solid line: model results; circles: measurements). In the panels are referred the day of the compared period.	17
3.6:	Distributions of tidal amplitude and phase for M_2 , S_2 , O_1 , K_1 , and M_4 harmonic constituents (black: model results, grey: measurements).	20
3.7:	Comparison between the relative amplitude errors obtained in this work and obtained by Oliveira <i>et al.</i> [2006a], for two stations (Cais do Bico and Costa Nova) of the Ria de Aveiro.	23
3.8:	Times series of current velocity at station I: a) zonal component; b) meridional component; c) intensity (solid line: model results; circles: measurements).	24
3.9:	Times series of current velocity at station J: a) zonal component; b) meridional component; c) intensity (solid line: model results; circles: measurements).	24
3.10:	Times series of current velocity at station K: a) zonal component; b) meridional component; c) intensity (solid line: model results; circles: measurements).	24
4.1:	Horizontal grid of Ria de Aveiro: a) Full grid with the red rectangle representing the study area. A, B and C are the selected areas where the velocities are represented; b) Detail of the grid in study area; c) Case Study 1; d) Case Study 2; e) Case Study 3; f) Case Study 4.	28

-
- 4.2: Magnitude of velocity in m/s during spring tide near the inlet of the lagoon (A in Figure 4.1). Above: a) Flood and b) ebb currents for the present bathymetry. Below: c) Flood and d) ebb currents for the case study 4. 29
- 4.3: Magnitude of velocity in m/s during spring tide (B in Figure 4.1). Above: a) Flood and b) ebb currents for the present bathymetry. Below: c) Flood and d) ebb for the case study 4. 30
- 4.4: Magnitude of velocity in m/s during spring tide (C in Figure 4.1). Left: a) Flood and b) ebb currents for the present bathymetry. Right: c) Flood and d) ebb for the case study 4. 31
- 4.5: Present bathymetry: a) Amplitude (m) distributions for the M_2 constituent; b) Phase ($^\circ$) distributions for the M_2 constituent; c) Amplitude (m) distributions for the M_4 constituent; d) Phase ($^\circ$) distributions for the M_4 constituent. 33
- 4.6: Case Study 4: a) Amplitude (m) distributions for the M_2 constituent; b) Phase ($^\circ$) distributions for the M_2 constituent; c) Amplitude (m) distributions for the M_4 constituent; d) Phase ($^\circ$) distributions for the M_4 constituent. 33
- 4.7: Asymmetric coefficients: Amplitude Ratio, Relative Phase ($^\circ$) and difference between ebb and flood duration (hours) along the axis of the four main channels of the Ria de Aveiro. (— Present Bathymetry, — Case Study 1, — Case Study 2, — Case Study 3 and — Case Study 4). 35
- 4.8: Cross-sections location, where the tidal prism were computed. 37
- 4.9: Computed tidal prism at 15 cross-sections of the Ria de Aveiro, at a) maximum spring tide, b) mean tide and b) minimum neap tide for the present bathymetry and for each case study. 38

List of Tabela

2.1:	Sample Stationa.	8
3.1:	Bottom friction coefficienta.	15
3.2:	RMS and Skill for all the calibration stationa.	18
4.1:	Total area and volume for each bathymetry and differencea in percentage.	27
4.2:	Magnitude of the maximum velocity in m/s in areaa A, B and C.	32
4.3:	Tidal prism for all the cross-sectiona for the present bathymetry and relative differencea for each case study and present bathymetry.	39

1. Introduction

1.1. Motivation and Aims

Coastal lagoons are saline water bodies separated or partially isolated from the sea. They may be enclosed by several barrier islands, like the Ria Formosa (in southern Portugal), as well as sand spits, or linked to the sea by one or more channels, which are small relative to the lagoon [Barnes, 1980], like the Ria de Aveiro (in northern Portugal).

The importance of lagoon systems and coastal water masses has been recognized a long time ago, not only by the scientific community, but also by the populations who live around these areas. Due to their interface location between land and open sea, and low depth, coastal lagoons are strongly submitted to natural constrains.

The Ria de Aveiro constitutes a very important area in the Portuguese west coast, with an adjacent surface of about 250 km². It is the most extensive shallow lagoon system in Portugal and the one most dynamic in terms of physical and biogeochemical processes. It has a very irregular geometry, being characterized by narrow channels and by the existence of intertidal areas, namely mud flats and salt marshes. The evolution of the Ria de Aveiro during the 20th century has been characterized by the erosion of mud flats, salt marsh and old salt pans, and widening of most channels. These changes together with other anthropogenic contributions are believed to have modified the tidal dynamics of the system, making it more vulnerable to risks of flooding and to sea level rise [da Silva and Duck, 2001].

The salt collecting activity in the Ria de Aveiro belongs to an old traditional activity fundamental to the regional economy, although it is decaying nowadays. The salt pans occupy almost 1500 ha, but a large number of them were abandoned and others were replaced by aquaculture tanks, as a consequence of the crisis affecting the sector, due to its low rentability. Moreover, the lack of maintenance due to the salt pans abandon, the strong flood currents inside the lagoon due to the frequent dredging operations in main channels and the wakes vessels, destroy the protector walls of the salt pans and excavates their bottoms. In fact, destruction of salt pans walls would result in a significant increase of the inundation area in Ria de Aveiro, and therefore it may affect the overall lagoon's hydrodynamic and the bottom morphology. An increase in the total area of the lagoon, as a result of intense destruction of salt pans walls would decrease the amplitude and increase the tidal phase inside the lagoon [Araújo *et al.*, 2008].

The primary aim of this work is to give a contribution to the understanding of the consequences of salt pans walls destruction, on the entire lagoon hydrodynamics. With this purpose, several

future scenarios were simulated, in which intense salt pans walls degradation was assumed. These simulations were performed through the shallow water numerical model ELCIRC (Eulerian-Lagrangian CIRCulation Model).

This study was developed in the framework of MURANO (Muros das Marinhas de Sal da Ria de Aveiro) project, which aims the salt pans walls rehabilitation in Ria de Aveiro lagoon. Hence this study may be a contribution to the development of a more realistic economic and effective strategy that allows salt pans protection and so mitigation of negative environmental impacts.

1.2. Structure of this work

This work is divided into five chapters. Chapter 1 presents the Introduction, where are described the motivation, aims and structure of the work and the state of the art. A detailed description of the salt field of Aveiro is given in Chapter 2, as well as is presented the field data and the location of the stations used in this study to calibrate the hydrodynamic model.

Chapter 3 contains the description of the hydrodynamic model and its establishment for the Ria de Aveiro lagoon. Hydrodynamic model calibration is also presented in this section. Chapter 4 includes the simulation of intense destruction of salt pans walls, which results in a significant increase of the inundation area in Ria de Aveiro, as well as in changes of the global and local hydrodynamic regimes, evaluated through the tidal prism and tidal asymmetry analysis. Results are discussed along all work and summarized in Chapter 5.

1.3. State of the Art

As previously referred, the importance of coastal environments is recognized all around the world by the scientific community. Several studies on coastal lagoons were published focusing on their hydrology, biology and ecological classification criteria [Battaglia, 1959; Barnes, 1980; Lasserre & Postma, 1982; Guelorget and Perthuisot, 1983; Bellan, 1987; Carrada & Fresi, 1988].

In the last 20-30 years the Ria de Aveiro lagoon was studied mainly from a biological and chemical point of view conducting to several publications like Cunha *et al.* [2001], Almeida *et al.* [2001] (bacterioplankton), Morgado *et al.* [2003] (zooplankton), Abrantes *et al.* [2006] (suspended sediments). A prior hydrological study reveals some of the main features of the Ria de Aveiro [Dias *et al.*, 1999]. According to this study the type of the tide at the mouth is semidiurnal and the tidal wave propagation in the lagoon has the characteristics of a damped progressive wave. They also concluded that the Ria de Aveiro should be considered as vertically homogeneous. Recent work [Araújo, 2005] has analysed sea level changes in Ria de Aveiro lagoon by comparing sea level elevations from two different surveys (1987/8 and 2002/3). These data were analysed by

harmonic analysis, and was concluded that there was a general increase in the amplitude and a phase decrease, for most of harmonic constituents. The tidal asymmetry also showed changes over the past years. During 1987/8, the majority of the lagoon was flood-dominant, since then, the central section of the lagoon has become ebb-dominant whilst the northern and southern sections are flood-dominant, i.e. presently there is no clear overall dominance. In this work, the influence of the increase of the inundation area in Ria de Aveiro lagoon, due to the salt pans walls destruction, will be studied through tidal asymmetry and tidal prism analysis.

The Ria de Aveiro has been also studied through numerical modelling. Several studies were performed to investigate topics such as the tidal propagation in the lagoon [Dias *et al.*, 2000; Dias and Fernandes, 2006], the Lagrangian transport of particles [Dias *et al.*, 2001] and sediment transport [Lopes *et al.*, 2001; Dias *et al.*, 2003; Lopes *et al.*, 2006].

Vaz *et al.* [2005], combining field measurements and modelling results, revealed the importance of the river flow in the establishment of the thermohaline horizontal patterns in the central area of the lagoon. A 3D baroclinic model (Mohid) is used by Vaz *et al.* [2007a], to perform hindcast simulations for the Espinheiro channel in Ria de Aveiro.

Oliveira *et al.* [2006a] uses the numerical model ELCIRC to analyze the tidal propagation in Ria de Aveiro lagoon and the variability of tidal asymmetry in the upper and lower lagoon. In this work, ELCIRC results were compared with observed values, as well as with results from the Ria de Aveiro hydrodynamics model developed previously by Dias *et al.* [2000] and Dias and Lopes [2006a, b], leading to the conclusion that the accuracy of ELCIRC is similar to the one of the referred model. Then sediment dynamics was studied through application of a morphodynamic modelling system and of a Lagrangian model.

According to Araújo *et al.* [2008] tidal changes in Ria de Aveiro lagoon show an average increase of 0.245 m in M_2 amplitude and 17.4 ° decrease in M_2 phase, over 16 years (1987-2004). This study investigates the causes of these changes using an analytical model and a hydrodynamic (vertically integrated) model. The analytical model provides a sensitive analysis of the response of the main tidal constituent, M_2 , to variations in: lagoon surface area, inlet channel depth and bottom friction. Although the analytical model treats the lagoon as a basin this sensitivity analysis provides an insight of possible sea level responses to these variations. However, results simulated using this approach are restricted by the analysis of independent effects of varying parameters when, in fact, they are known to be dependent on each other. There is also the limiting assumption that levels in the lagoon rise and fall in unison. These restrictions imposed by the analytical model are overcome using the hydrodynamic numerical model. The hydrodynamic model is used to evaluate whether changes in bathymetry are reflected in the tidal characteristics of the lagoon. Both approaches

confirm that changes in the bathymetry of the inlet channel are the most significant contribution to the tidal changes. Taking into account the restrictions of the analytical models, in the present work a numerical hydrodynamic model was applied in Ria de Aveiro. The numerical simulations were performed to evaluate the changes in the amplitude and phase of M_2 and M_4 constituents in conditions of salt pans walls destruction that leads to an increase of the inundation area. The phase of M_4 relative to M_2 and the amplitude ratio $A_r = A_{M_4} / A_{M_2}$ were also evaluated, in order to analyse the changes in tidal asymmetry.

During the last years, a huge effort was placed in the implementation of numerical models that resolve the main physical processes occurring in estuarine systems. Several estuarine modelling studies have considered one dimensional (vertical) representations of the velocity and salinity fields [Nunes Vaz *et al.*, 1989; Simpson *et al.*, 1990; 1991; Nunes Vaz and Simpson, 1994; Monishmith and Fong, 1996]. Warner *et al.* [2005] have used ROMS [Haidvogel *et al.*, 2000] in order to evaluate the estuarine dynamics of the Hudson estuary, providing a skill assessment of the model by comparison of model results and observed data. The dynamics of Chesapeake Bay has been studied using ROMS [Li *et al.*, 2005]. The same model was used by Zhong and Li [2006] to compute tidal energy fluxes and dissipation in Chesapeake Bay. A combination of three-dimensional numerical model GETM (General Estuarine Transport Model) [Burchard and Boldin, 2002; Burchard *et al.*, 2004] results with data analysis and used by Stanev *et al.* [2003] to gain a better understanding of the major characteristics of the circulation in the East Frisian Wadden Sea.

In this work the shallow water model ELCIRC was implemented in Ria de Aveiro lagoon. ELCIRC is a fully non-linear, three dimensional, baroclinic shallow water model which is being developed as an open source community model at the Center for Coastal Margin Observation and Prediction [Zhang *et al.*, 2004]. The model ELCIRC was been applied by several authors, such as Baptista *et al.* [2004], Oliveitra *et al.* [2006b], Oliveira *et al.*, [2006c] and Dias [2009].

2. The Study Area

2.1 Description of the study area

The Ria de Aveiro (Figure 2.1) is a shallow mesotidal lagoon located in Northwest coast of Portugal (40°38'N, 8°44'W). The lagoon has a maximum width of 10 km and its length measured along the longitudinal axis is 45 km [Dias and Lopes, 2006a]. The average depth of the lagoon relative to the local datum is about 1 m, except in navigation channels where dredging operations are frequently carried out. Due to the small depth and to the significant tidal wave amplitude there are zones, especially along the borders of the lagoon and its central area, which are alternately wet and dry during each tidal cycle.

Although several rivers discharge into the Ria de Aveiro, the most important freshwater contribution is from Vouga (50 m³s⁻¹ average flow) and Antuã (5 m³s⁻¹ average flow) rivers [Moreira *et al.*, 1993]. Vouga River is responsible by approximately 2/3 of the freshwater input into the lagoon [Dias *et al.*, 1999]. The tides at the mouth of the lagoon are predominantly semidiurnal (M_2 constituent dominance), with a mean tidal range of about 2.0 m. The minimum tidal range is 0.6 m (neap tides), and the maximum tidal range is about 3.2 m (spring tides), corresponding to a maximum and a minimum water level of 3.5 and 0.3 m, respectively [Dias *et al.*, 2000].

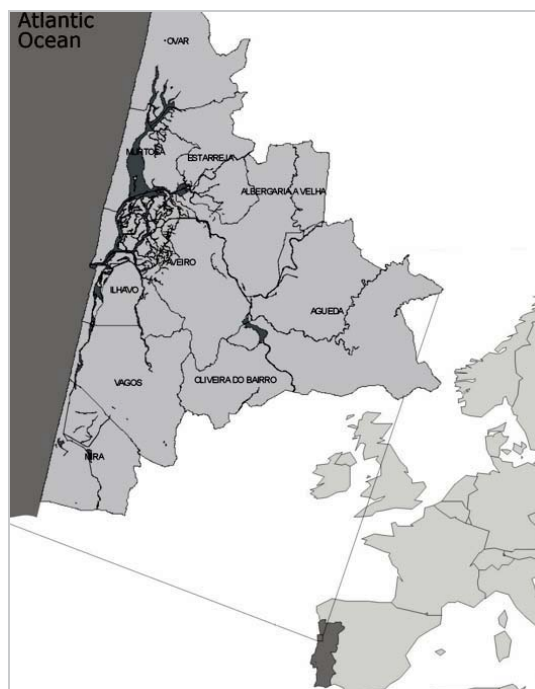


Figure 2.1: Ria de Aveiro lagoon.

According to Dias [2001], the estimated tidal prism of the lagoon is $136.7 \times 10^6 \text{ m}^3$ for a maximum spring tide and $34.9 \times 10^6 \text{ m}^3$ for minimum neap tide. The total estimated freshwater input is very small (about $1.8 \times 10^6 \text{ m}^3$ during a tidal cycle) [Moreira *et al.*, 1993] when compared with the mean tidal prism at the mouth of the lagoon (about $70 \times 10^6 \text{ m}^3$), indicating that the lagoon may be vertically homogeneous in terms of salinity.

A prior hydrological characterization led to the conclusion that the Ria de Aveiro can be considered vertical homogeneous during dry seasons. However, after important rainfall the stratification becomes important near the freshwater inflow locations [Dias *et al.*, 1999].

There is a small artificial headland (Triângulo Divisor das Correntes) dividing the entrance channel in two different arms. Due to this feature the tidal prism of a flowing tide is separated in two flows: a small one flowing into Mira channel and a second more important one flowing to the other channels, namely S. Jacinto and Espinheiro channels [Dias, 2001]. The tidal prism in each one of the main channels relative to its value at mouth is about 38% for S. Jacinto channel, 26% for Espinheiro channel, 10% for Mira channel and 8% for Ílhavo channel [Silva, 1994]. According to Dias [2001] this values are about 35.4% for S. Jacinto channel, 25.6% for Espinheiro channel, 10.0% for Mira channel and 13.5% for Ílhavo channel.

Morphologically, the Ria de Aveiro lagoon has been shaped recently. The lagoon began its geological formation in the 10th century, and in the 17th century the water mass is completely isolated, leading to the artificial opening of the present mouth in the central area of the lagoon in 1808 [Abecasis, 1961]. The present configuration of the Ria de Aveiro is essentially function of the hydrodynamic processes driving the transport, erosion and deposition of sediments. The human action is also being another determinant factor in this evolution, especially since the intervention to artificially fix the sea entrance and the consequent works in the harbour and entrance channels [Dias, 2001].

The salt field of Aveiro occupies about 1500 ha, at the Concelho de Aveiro and Ílhavo. In 15th century there were 500 active salt pans, fifty years ago about 270 salt pans produced salt and in 2006 were only eight. The salt pans currently occupy the marsh areas, which are islands in the lagoon and only few have access by land [INTERREG IIIB, 2008].

Figure 2.2 shows a satellite image of the Ria de Aveiro lagoon, covering salt pans separated by channels, divided into five groups [INTERREG IIIB, 2008]:

1. Grupo de São Roque ou Esgueira - near the urban shavings of Aveiro, and separated from it by the São Roque channel, limited to North and West by the Cale da Veia and East by the Esteiro de Esgueira;

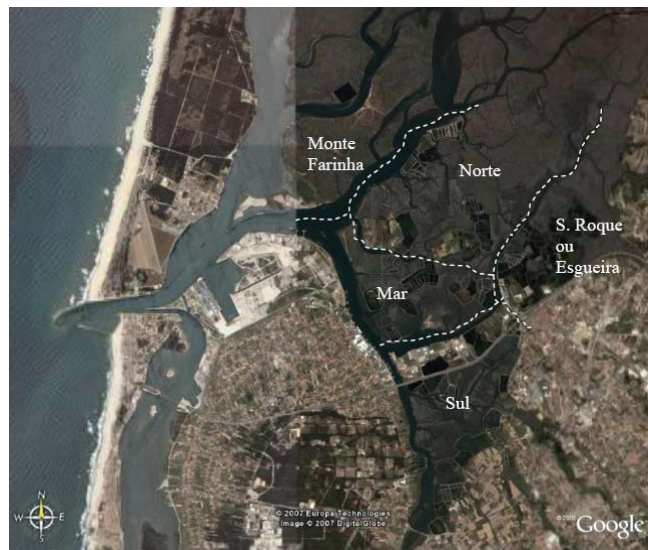


Figure 2.2: Salt pans of the Ria de Aveiro lagoon.

2. Grupo do Sul - south of the main channel that communicates with the Canal das Pirâmides until the Cale da Gafanha, limited to the West by the Canal de Ílhavo, to East by the Canal das Pirâmides and to South by Ílhavo;
3. Grupo do Mar - north of the main channel and south of the Esteiro de Sama, limited to the East by the Cale da Veia and to the West by the Cale da Gafanha or the Canal da Cidade;
4. Grupo do Norte - between the Cale do Espinheiro and the Rio Novo, limited to North and West by the Esteiro de Sama, to South by the Cale dos Bulhões and to East by the Cale da Veia;
5. Grupo do Monte Farinha - between the Cale de Oiro and Parrachil to North, the Cale do Espinheiro and the Rio Novo to East and South, and the Cale de Oiro and Cale da Gaivota to West.

Due to the large extension of the salt field of Aveiro, it is impossible to perform an integrate study of all salt pans. Therefore, this work will focus in the Grupo do Mar and south of the Grupo do Norte, that are the most vulnerable to the strong currents.

2.2 Field Data

Data available for this study are from two distinct field campaigns, one realized in 2003 and the other in 2006 and are summarized in Table 2.1. Sea surface elevation and vertical profiles of current were collected, in the framework of SAL project – Sal do Atlântico (UE – INTERREG III B Espaço Atlântico) [2004-2007], at stations P1, P2 and P3 (near the salt pans) and were available for this study. For these stations data was measured hourly.

Measurements of sea surface elevation for the other stations presented in Table 2.1 were measured every six minutes, except for Torreira station where measurements were performed every half hour. These data were collected in the framework of the Phd Thesis of Araújo [2005].

Table 2.1: Sample Stations.

Station	Latitude (N)	Longitude (W)	Start	End
Barra	40°38'34.1''	08°44'51.8''	01-04-2003 (0:05:09)	01-05-2003 (0:05:09)
S. Jacinto	40°39'37.4''	08°43'30.9''	12-12-2003 (0:00:00)	01-01-2004 (0:00:00)
Cires	40°39'30.0''	08°42'36.0''	08-08-2003 (0:01:27)	07-09-2003 (0:01:27)
Lota	40°38'41.8''	08°39'42.4''	07-03-2003 (0:02:05)	06-04-2003 (0:02:05)
Ponte Cais 2	40°38'15.6''	08°41'26.2''	08-08-2003 (0:05:50)	07-09-2003 (0:05:50)
Costa Nova	40°37'06.0''	08°44'48.0''	08-05-2003 (0:00:00)	08-06-2003 (0:00:00)
Torreira	40°45'36.2''	08°41'39.4''	08-08-2003 (0:00:00)	07-09-2003 (0:00:00)
Vagueira	40°33'36.0''	08°45'21.7''	09-05-2003 (0:00:30)	08-06-2003 (0:00:30)
P1	40°39'01.2''	8°39'58.8''	22-05-2006 (08:52:00)	22-05-2006 (20:49:00)
P2	40°38'57.0''	8°39'51.7''	22-05-2006 (09:04:00)	22-05-2006 (20:54:00)
P3	40°38'41.4''	8°39'54.0''	22-05-2006 (09:17:00)	22-05-2006 (21:00:00)
Cais do Bico	40°43'36.0''	08°38'48.0''	13-06-2003 (0:03:31)	13-07-2003 (0:03:31)
Vista Alegre	40°36'06.7''	08°41'01.5''	10-09-2003 (0:01:04)	10-10-2003 (0:01:04)
Cacia	40°41'36.2''	08°35'59.8''	07-03-2003 (0:04:55)	06-04-2003 (0:04:55)

The bathymetric data (Figure 2.3) available for this study was collected in a general survey carried out in 1987/88 by the Hydrographic Institute of Portuguese Navy [IH]. Dredging operations performed in 1998 in Mira and S. Jacinto channels and as well as data from recent surveys performed by the Administração do Porto de Aveiro close to the lagoon mouth. For these regions the original values of water depth were replaced by the recent ones. In Figure 2.3 were also presented the location of stations referred in Table 2.1. Although more data were available for other stations, were not considered in this study due to the location of preferential study area.

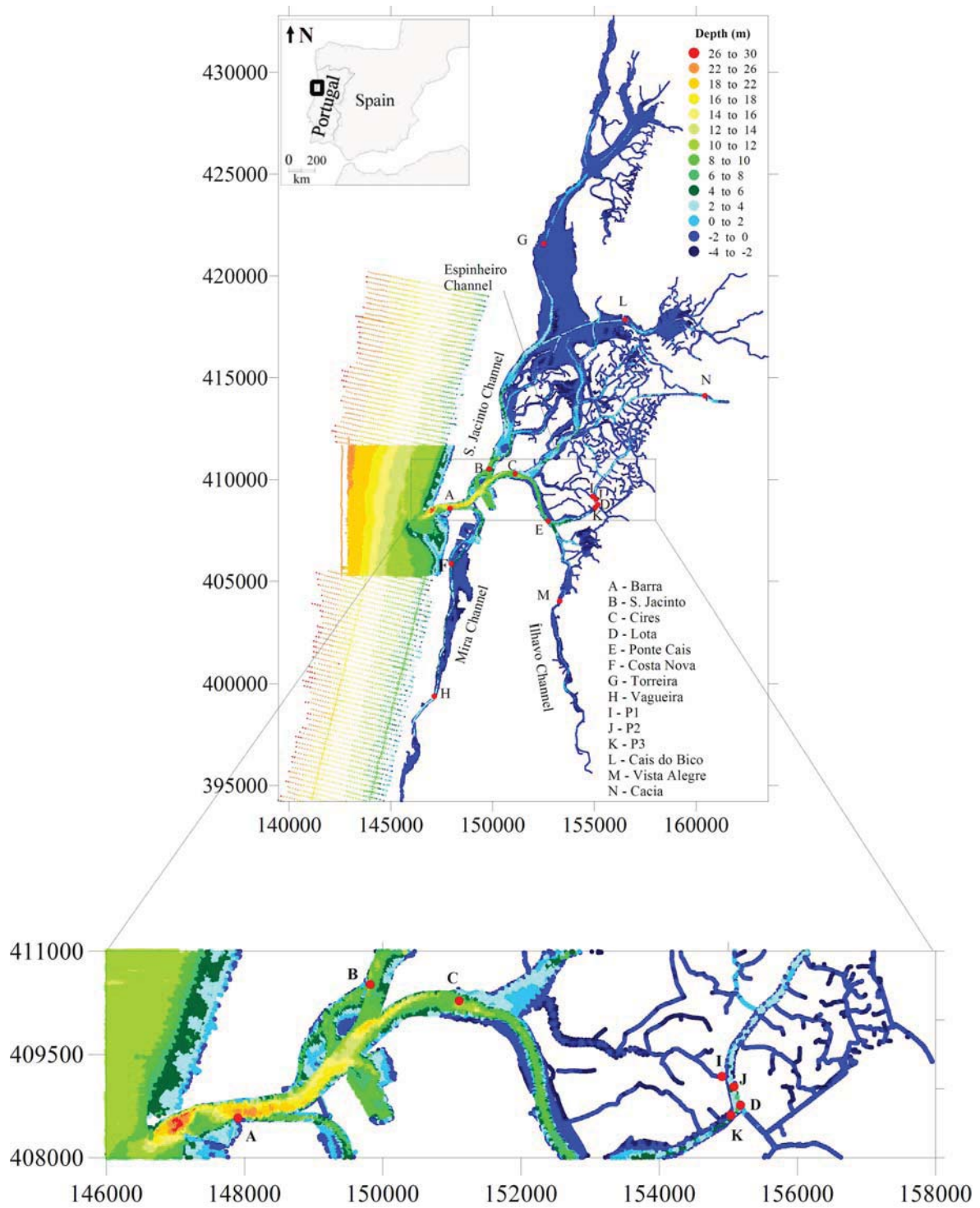


Figure 2.3: Ria de Aveiro bathymetry, represented in UTM coordinates, with depth in meters relative to the hydrographic null (-2.00 m below mean sea level) and with locations of the stations where field data is available.

3. Numerical model

3.1. Model Description

ELCIRC is a model designed for the effective simulation of three dimensional baroclinic circulation across river-to-ocean scales. The model ELCIRC uses a finite-volume/finite difference Eulerian-Lagrangian algorithm to solve the shallow water equations, written to realistically address a wide range of physical processes and of atmospheric, ocean and river forcings [Zhang *et al.* 2004]. The equations are solved with a finite volume technique conservation and natural treatment of wetting and drying. The horizontal domain is discretized with a triangular mesh for flexibility, and z-coordinates are used in the vertical. A semi-implicit time-stepping algorithm and the Lagrangian treatment of the advective terms ensure stability at large time steps [Oliveira *et al.* 2006a].

ELCIRC is able to determine the free surface elevation, 3D water velocity, salinity and temperature, using a set of six hydrodynamic equations based on the Boussinesq and hydrostatic approximations, which represent mass conservation, momentum conservation, and conservation of salt and heat. In the present work is used only the hydrodynamic module of this model.

For the Aveiro lagoon model, a single vertical layer is used, so ELCIRC reverts to two dimensions. Due to the shallow depths and minor freshwater inputs of this system, circulation can adequately be simulated with a depth-averaged model.

The depth-integrated equations solved in this model express the conservation of mass and momentum:

$$\frac{\partial \eta}{\partial t} + \frac{\partial [HU]}{\partial x} + \frac{\partial [HV]}{\partial y} = 0 \quad 3.1$$

$$\frac{\partial U}{\partial t} + U \frac{\partial U}{\partial x} + V \frac{\partial U}{\partial y} = fV - g \frac{\partial \eta}{\partial x} - \frac{\tau_x}{\rho} + \varepsilon \left(\frac{\partial^2 U}{\partial x^2} + \frac{\partial^2 U}{\partial y^2} \right) \quad 3.2$$

$$\frac{\partial V}{\partial t} + U \frac{\partial V}{\partial x} + V \frac{\partial V}{\partial y} = -fU - g \frac{\partial \eta}{\partial y} - \frac{\tau_y}{\rho} + \varepsilon \left(\frac{\partial^2 V}{\partial x^2} + \frac{\partial^2 V}{\partial y^2} \right) \quad 3.3$$

where $H(x, y) = h(x, y) + \eta(x, y, t)$ is the water height, η is the surface water elevation, $h(x, y)$ is the water depth, g is the acceleration of gravity, t is the time, U and V are the depth-average velocity components in the x (eastward) and y (northward) direction, ρ is the water density, ε is the horizontal eddy viscosity, τ_x and τ_y are the bottom stress according to each horizontal direction and are defined in the following form:

$$\tau_x = \rho C_D \sqrt{U^2 + V^2} U \quad 3.4$$

$$\tau_y = \rho C_D \sqrt{U^2 + V^2} V \quad 3.5$$

where C_D is the drag coefficient and ρ is the reference density. The friction between the interface ocean-atmosphere was not considered in this work.

The earth rotation is represented through the Coriolis acceleration in the momentum equations. The Coriolis factor, f , is a well known function of latitude ϕ :

$$f(\phi) = 2\Omega \sin \phi \quad 3.6$$

where $\Omega = 7.29 \times 10^{-5}$ rad/s. Due to the relatively reduced dimension of the domain in the N-S direction, a constant Coriolis factor was used ($f = 0.000093$ rad/s).

In this work was used an ELCIRC version that applied the Manning law with a space varying friction coefficient. Thus, the bottom drag coefficient present in Equations 3.4 and 3.5 can be expressed as:

$$C_D = gn^2 H^{-\frac{1}{3}} \quad 3.7$$

where n is the Manning coefficient.

The numerical algorithm of ELCIRC used a semi-implicit scheme. The barotropic pressure gradient in the momentum equation and the flux term in the continuity are treated semi-implicitly, with implicitness factor $0.5 \leq \theta \leq 1$. The vertical viscosity term and the bottom boundary condition for the momentum equation are treated fully implicit and all other terms are treated explicitly. According to Casulli and Cattani [1994] this ensures both stability and computational efficiency.

3.2. Model Establishment

As previously referred, ELCIRC was already implemented successfully in Ria de Aveiro, in order to study its inlet dynamics in terms of tidal propagation, as well as the variability of tidal asymmetry in the upper and lower lagoon [Oliveira *et al.*, 2006a]. In this work was used a horizontal grid with 29380 elements and 18851 nodes, which includes an area of about 206 km² (Figure 3.1 a)). In fact, this horizontal grid reveals insufficiently for the present work because many channels are not represented, mainly in the central zone. For that reason and taking into account the main aim of this work there was a need to complete the existing grid, adding and refining several channels, mainly in the central zone of the lagoon, where salt pans are located. The final grid includes an area of about 210 km² (Figure 3.1 b)), has 94352 elements and 71996 nodes. In Figure 3.2 a detail of both grids near the study area was represented.

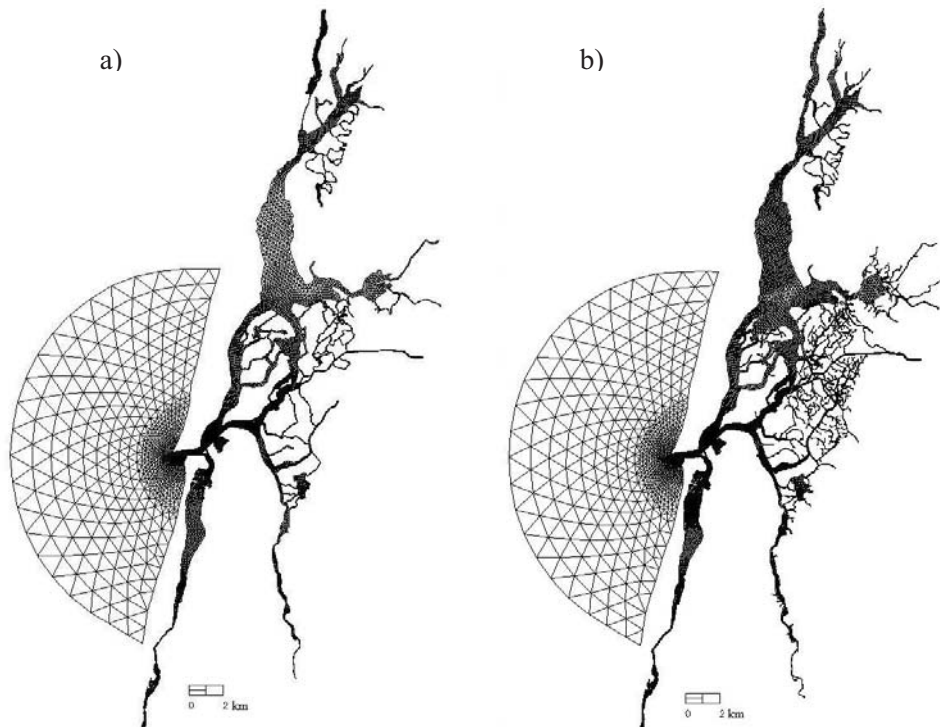


Figure 3.1: Horizontal grid of the Ria de Aveiro: a) Old grid; b) New grid.

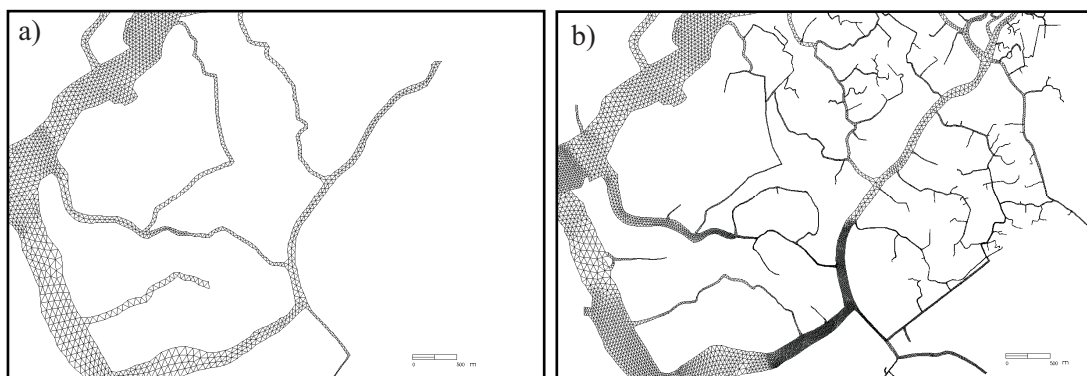


Figure 3.2: Detail of the grid near the study area: a) Old grid; b) New grid.

The generation of the new grid was made using the semi-automatic software for generation of two-dimensional finite elements grids XMGREDIT [Turner and Baptista, 1993]. This task was meticulous and enormously time consuming due to several aspects, such as the lagoon complex geometry, the narrow channels that characterize the Ria de Aveiro lagoon and the huge lack of channels in the lagoon central area. In order to generate a grid which adequately represents the channels dimensions it was necessary to recur to Google Earth that allowed the determination of the channels width and length. Moreover, in the improving of the grid was necessary to take into account that each node was not connected to more than 7 elements and check the orthogonally and limit maximum angles to 90° . The grid resolution varies from about 0.5 km near the open boundary

to about 1 m in the narrow channels. The computational domain extends from the upstream limits of the lagoon to the continental shelf.

The hydrodynamic model ELCIRC was forced by fourteen harmonic constituents (Z_0 , M_{SF} , O_1 , K_1 , N_2 , M_2 , S_2 , M_4 , MN_4 , MS_4 , M_6 , K_2 , P_1 and Q_1) taken from the regional model of Fortunato *et al.* [2002], without any wind and freshwater input. The largest time step that prevents the appearance of oscillations was set to 90 s. The initial conditions of levels and velocities were specified from the repose and a ramp function of 1 day was used.

Probably, the most important factor that affects the flow in a shallow water system like the Ria de Aveiro lagoon is the numerical bathymetry. The numerical bathymetry, referent to average mean sea level (2 m), is presented in Figure 3.3, as well as the location of the stations used in the hydrodynamic model calibration.

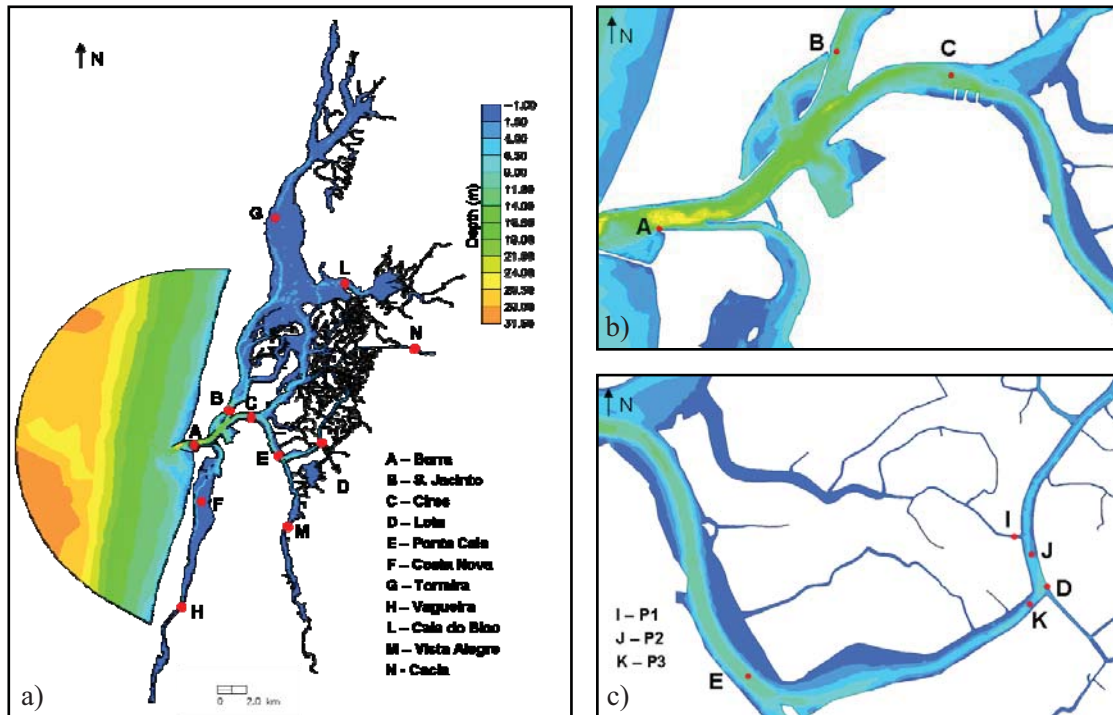


Figure 3.3: Ria de Aveiro lagoon numerical bathymetry, with depth in meters relative to the mean sea level (2 m) and with the locations of the stations used in the calibration of the numeric model: a) Entire lagoon; Detail of bathymetry near the inlet b) and near the study area c).

3.3. Hydrodynamic Model Calibration

Nowadays, numerical models are used as sophisticated techniques of interpolation and extrapolation of field data in both spatial and temporal domains. On the other hand, realistic model results cannot be obtained without adequate supporting data. It is an accepted requirement that a

numerical model of estuarine hydrodynamics should be calibrated and validated before used in a practical application. However, the procedures to perform these tasks are not widely accepted [Cheng *et al.*, 1991]. Calibration and validation methods appear in several forms, depending on data availability and researchers opinion [Hsu *et al.*, 1999]. The model calibration is based on the determination and the adjustment of parameters to which the model is most sensitive. In case of hydrodynamic modelling, the calibration is frequently made by qualitative comparison of time series of predicted and measured data for the same location and period of time [Cheng *et al.*, 1993]. Another method used consists in comparing the harmonic constituents generated from predicted and observed data. The model validation is the procedure of comparing the model output with available data to prove the model skill under different conditions [Dias *et al.*, 2009]. The measurements used to perform the validation have to be independent from the data set used for calibration.

In this work model calibration was carried out by comparing model results with observed sea surface elevation (SSE) and by comparing the amplitude and phase of the harmonic constituents.

Calibrations were conducted for two distinct parameterizations of friction: a constant Manning coefficient and a depth dependent Manning coefficient, following the relationship showed in Table 3.1. Thus, it was decided to use a depth dependent Manning coefficient, because the water depth strong influences the bottom stress. The Manning coefficients were adjusted using the guide principle that an increase in the bottom friction will produce a decrease in the tidal wave in that zone of the channel and in the channel's upstream. Another principle used is that an increase in the bottom roughness will produce an increase in the phase lag for high tide and a decrease for low tide [Fry and Aubrey, 1990]. The Manning values used to calibrate the hydrodynamic model were based on the values presented by Dias [2001] for the Ria de Aveiro and were adapted in order to achieve a good calibration.

Table 3.1: Bottom friction coefficients.

Depth (m)	Manning's n values
$-1 \leq h < -0.5$	0.026
$-0.5 \leq h < 0.0$	0.024
$0.0 \leq h < 0.5$	0.022
$0.5 \leq h < 1.0$	0.020
$1.0 \leq h < 3.0$	0.018
$3.0 \leq h < 6.0$	0.016
$6.0 \leq h < 10.0$	0.015
$h \geq 10.0$	0.014

The calibration was performed at 14 stations within the lagoon (Figure 3.3). However, the comparison between the predicted and observed time series of sea surface elevation is shown, in Figures 3.4 and 3.5, only for some stations. Due to the limited space only stations near the lagoon mouth and near the study area are represented. The hydrodynamic model was forced in the oceanic boundary by tides only, so in order to compare model results with measurements, the low frequency signal was removed from the data, considering a cut-off frequency of 0.0000093 Hz (30 h).

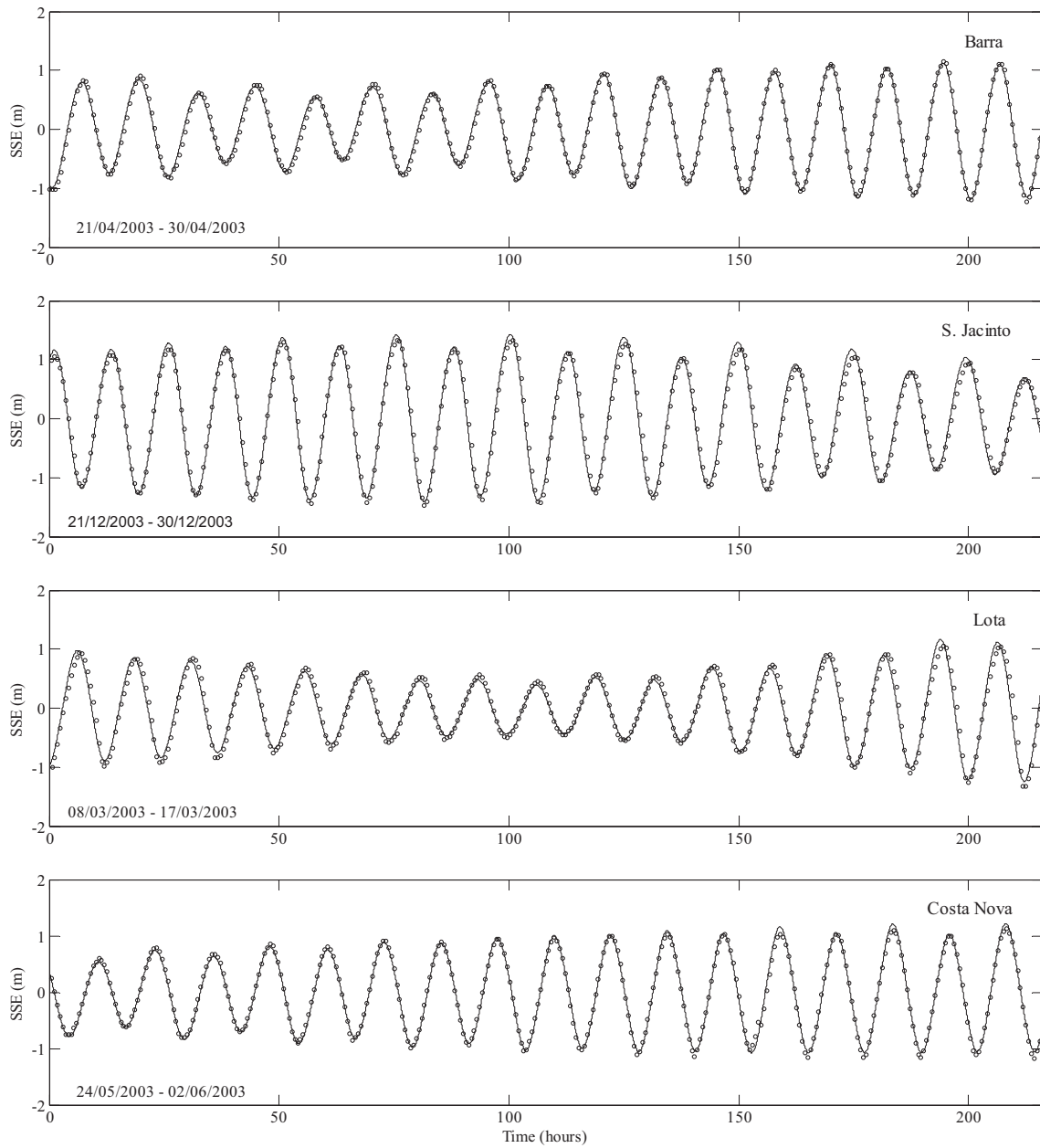


Figure 3.4: Comparison between predicted and observed sea surface elevation (solid line: model results; circles: measurements). In the panels are referred the beginning and the end of each compared period.

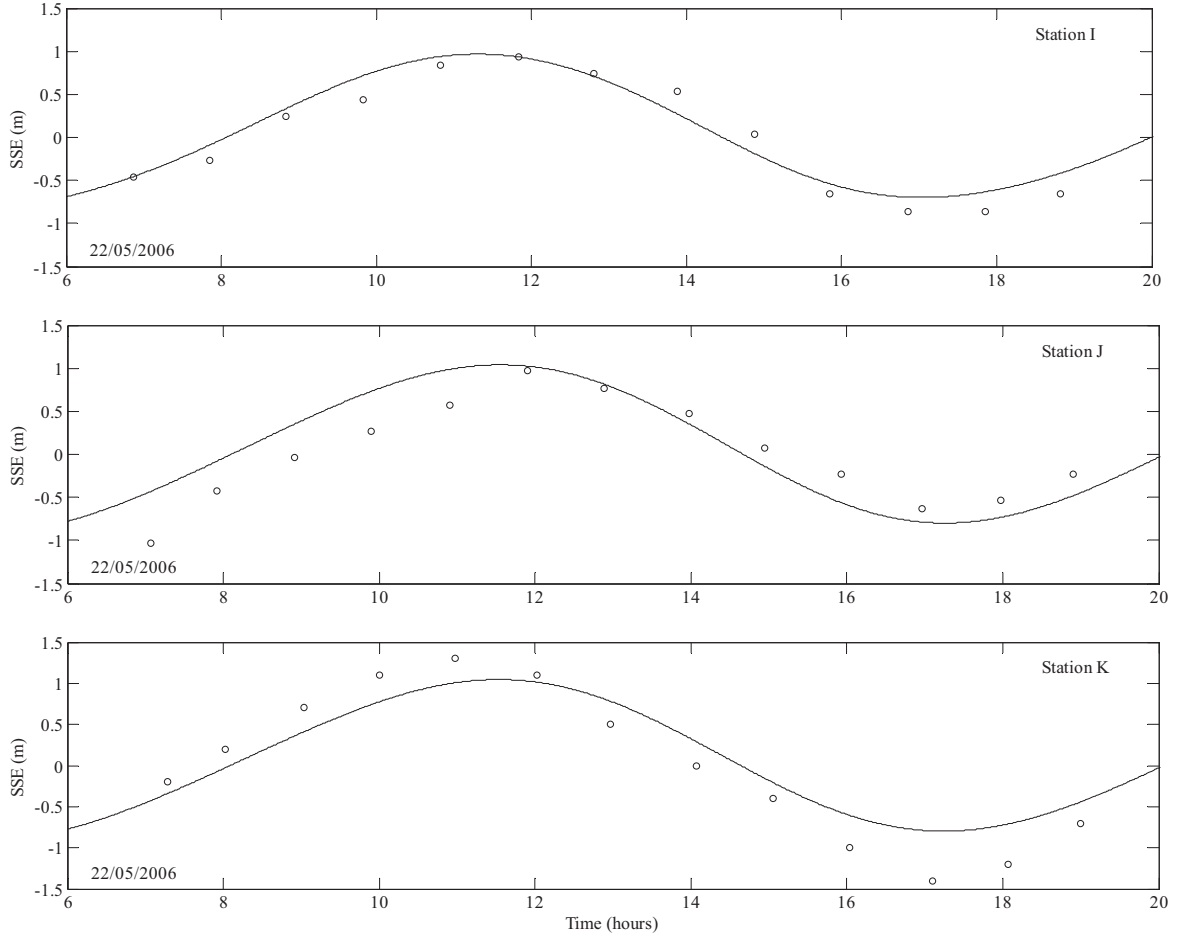


Figure 3.5: Comparison between predicted and observed sea surface elevation (solid line: model results; circles: measurements). In the panels are referred the day of the compared period.

The model performance in the reproduction of the SSE was measured by RMS error between computed and observed data:

$$RMS = \left\{ \frac{1}{N} \sum_{i=1}^N [\zeta_0(t_i) - \zeta_m(t_i)]^2 \right\}^{\frac{1}{2}} \quad 3.8$$

where $\zeta_0(t)$ and $\zeta_m(t)$ are the observed and computed SSE, respectively and N is the number of measurements in the time series. According to Dias *et al.* [2009] the RMS values should be compared with the local tidal amplitude. If they are lower than 5% of the local amplitude, the agreement between model results and observations should be considered excellent. If they range between 5% and 10% of the local amplitude the agreement should be considered very good.

The model predictive Skill it was also computed that is based on the quantitative agreement between model results and observations [Warner *et. al.*, 2005]:

$$Skill = 1 - \frac{\sum |\zeta_m - \zeta_o|^2}{\sum [|\zeta_m - \bar{\zeta}_o| + |\zeta_o - \bar{\zeta}_o|]^2} \quad 3.9$$

where ζ is sea surface elevation and $\bar{\zeta}$ the time mean. Perfect agreement between model results and observations will yield a skill of one and complete disagreement yield a skill of zero. Skill values higher than 0.95 should be considered representative of an excellent agreement between model results and observations [Dias *et al.*, 2009].

The RMS and Skill were computed for each station and are summarized in Table 3.2.

Table 3.2: RMS and Skill for all the calibration stations.

Station	RMS (m)	Skill
A	0.0759	0.9928
B	0.0924	0.9904
C	0.1680	0.9864
D	0.2273	0.9789
E	0.1499	0.9764
F	0.0856	0.9928
G	0.2583	0.8244
H	0.3297	0.7764
I	0.1443	0.9661
J	0.2476	0.8042
K	0.1927	0.9468
L	0.3250	0.7295
M	0.3357	0.9177
N	0.2542	0.9709

The RMS values range from 3% to 10% of the local amplitude for the stations A, B, C, E, F, I and K, and therefore the predictions and observations agreement ranges from very good to excellent. However, for the other stations the RMS values are higher than 10% of the local amplitude.

The agreement between computed and observed data at station A should be perfect because this station is the nearest of open boundary. In fact, the open boundary was forced by 14 constituents, whose values were obtained by the interpolation of amplitude and phases from the regional tidal model of the Atlantic Iberian shelf of Fortunato *et al* [2002]. The regional model was validated with velocity and elevation data from several stations along the western Iberian coast. However, the regional model has a low resolution near the oceanic boundary, which may be leads to the errors found in station A.

A RMS error of about 7 cm was found for the station located at the lagoon mouth. This difference represents less than 4% of the mean tidal range near the mouth of the lagoon. Thus, the errors found in the other stations may be partially explained by this difference. The best model results were obtained for the stations closer to the lagoon's mouth (e.g. S. Jacinto station with a RMS of 9 cm) and the highest disagreements were found for stations G, H and L with RMS errors around 15% of tidal range and with skill values lower than 0.95. At station N (Cacia) a RMS error of about 25 cm was found, that may be due to several factors, such as the distance to the lagoon mouth, which is about 12 km, the fact that this station is placed close the Vouga River mouth and freshwater input was not considered in the model, or the small depth of the channel (~2 m). Relatively to the stations located in central area of the lagoon, the comparison between predicted and observed SSE, shown in Figure 3.5, reveals that the model is slightly advanced relatively to the data for stations I and J. Consequently, RMS errors of about 14 cm and 24 cm were found for stations I and J, respectively. At station K model amplitude is lower than the observed and a RMS of 19 cm was found. These three stations are very important because they are located in the salt pans surrounding channels and it is relevant for the present work that the model accurately reproduces the tide propagation in this zone. Although the only data available for these stations were measured every hour during 11 hours, it can be considered that the model reproduces well the SSE.

There is a large disadvantage on the direct comparison of RMS and Skill errors, since phase and amplitude errors are considered together. Thus, harmonic analysis was computed for both predicted and observed SSE in order to quantify separately the amplitude and phase differences for all stations, with exception of I, J and K stations because the available data for these stations only have the duration of 11 hours. This procedure was performed using *t_tide* matlab® package of Pawlowicz *et al.* [2002].

Results for the major semidiurnal and diurnal tidal constituents (M_2 , S_2 , O_1 , K_1) are presented in Figure 3.6, as well as for the shallow water constituent, M_4 .

The agreement between predicted and observed values is good both in amplitude and in phase for the semidiurnal constituents, which are the major tidal constituents in Ria de Aveiro. For M_2 constituent, which amplitude is the highest one, the mean difference between predicted and observed amplitudes is about 10 cm. This value was amplified by the errors found for stations G, H and L, that presents a mean difference of about 16 cm. If the values for these stations are not considered, the mean difference between predicted and observed amplitudes is about 4 cm.

For S_2 constituent the mean difference between predicted and observed amplitude is about 3 cm. In fact, the model results represent the amplitude of S_2 constituent, for the stations G, H and L,

more accurately than the amplitude of M_2 constituent, which attenuate the S_2 amplitude mean difference.

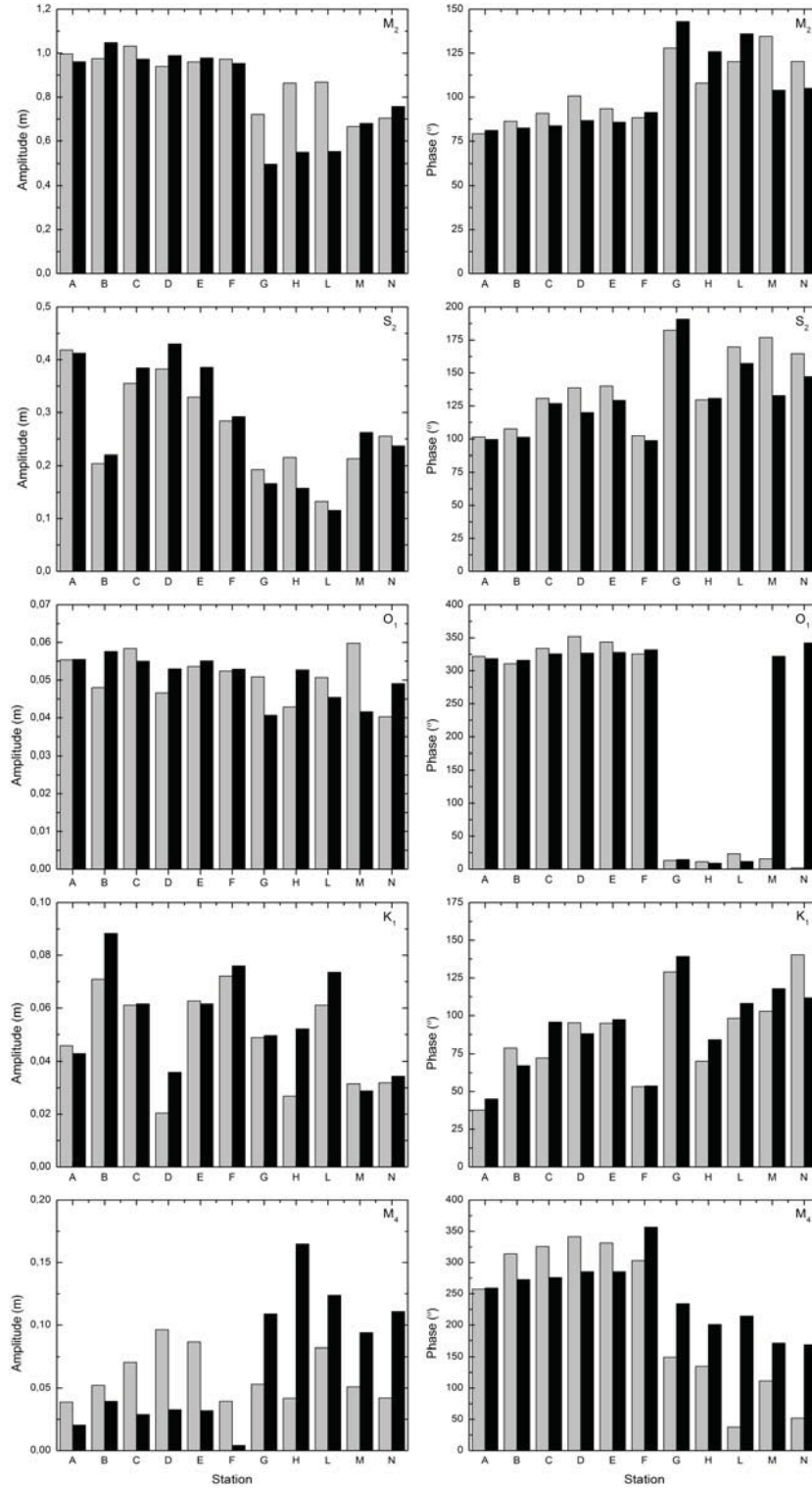


Figure 3.6: Distributions of tidal amplitude and phase for M_2 , S_2 , O_1 , K_1 , and M_4 harmonic constituents (black: model results, grey: measurements).

The mean phase difference for both semidiurnal constituents is about 12° , which means that the average delay between the predicted and observed tide is about 24 minutes. This delay is bigger than was expected, mainly due to the phase difference at stations L and M. At station M (Vista Alegre) the phase difference is about 30° (60 minutes) for M_2 constituent and 40° (80 minutes) for S_2 , which can be explained by the strong constriction that exists in the channel, with a width of about 10 m, where very strong currents occur.

No justification was found for the errors determined for station G (Torreira) and L (Cais do Bico). Despite the strong effort to diminish errors, it was not possible to improve the agreement between predicted and observed data in these stations without deteriorating the results for the other stations.

At station H (Vagueira) the difference between predicted and observed phase was about 17° for M_2 constituent, which corresponds to an average delay of about 35 minutes and the amplitude difference is about 31 cm (~36% of constituent amplitude). This station is located in Mira channel, a large channel, however most water passes through a narrow space. This feature is not recognized by the model, so it cannot reproduce the reality very well. This situation could be adjusted by refining the mesh along the main channel, however, the study area is far and not influenced by this channel, so it was decided that the error obtained in this station is not relevant. Therefore it is difficult to improve the model results in this channel without increasing to much the computational effort.

For the diurnal constituents (O_1 and K_1) the agreement may be considered good for all stations. However, it was found an amplitude error of about 25% at station G and about 43% at station M for O_1 constituent. For K_1 constituent the major amplitude error was around 45% at stations D and H.

For M_4 constituent the mean difference between model results and observed amplitude is about 5 cm. At station A the model reproduces the phase of M_4 constituent very well, with a difference less than 2° , which represents an average delay of about 1 minute. However the amplitude of this constituent is not so well reproduced by the model. In fact, an amplitude error of about 47% was found in this station. The differences in both amplitude and phase for this constituent increases with the distance to the lagoon mouth. In general, the amplitude of this constituent along the Ria de Aveiro is higher than at the mouth, indicating that this frequency is generated inside the lagoon.

The M_4 constituent was not simulated with the expected accuracy. The errors found in the M_4 reproduction may be due to bathymetric errors that can not be corrected by the adjustment of the bottom coefficient. Moreover, according to Araújo *et al.* [2008] an average increase of 0.245 m in M_2 amplitude and an average 17.4° decrease in M_2 phase, over the 16 years were observed. As the bathymetric data and the water level field data used to calibrate the model were measured with the

time gap of 16 years referred by Araújo *et al.* [2008] (bathymetric data was mainly collected in 1987/88 while the field data used in the M_4 calibration was collected in 2003) the errors in M_2 amplitude will induce errors in M_4 amplitude. Nevertheless, if M_2 amplitude changes 0.245 m in 16 years, M_4 will also change, since the M_2 energy is almost all transferred to M_4 . However, as the M_4 constituent is generated through the non-linear interactions in the equations of motion and continuity, which are generally well adjusted by the model, the results for M_4 are considered accurate enough to perform this study.

From observation of SSE data and harmonic analysis it is concluded that friction dissipates energy as the tidal wave propagates landward from the lagoon mouth. This behaviour is a common feature in estuarine environments [Hsu *et al.*, 1999].

The results from the harmonic analysis show that constituents M_2 and S_2 together determine about 90% of the astronomic tide in Ria de Aveiro, in accordance with previous studies [Dias *et al.*, 1999; 2000]. Harmonic analysis of sea surface elevation also reveals that the oceanic tide is semi-diurnal (Form Number ≈ 0.07).

Thus, it is concluded that the hydrodynamic model calibration was successfully achieved, although the differences between model and field data exist.

In order to evaluate the influence of the new bathymetry in the model's accuracy in reproducing the Ria de Aveiro lagoon hydrodynamics, some comparisons between the model results obtained in this work and those obtained by Oliveira *et al.* [2006a] were performed. Thus, the relative amplitude errors for the M_2 , S_2 , K_1 and O_1 constituents at stations L and F were compared and are presented in Figure 3.7. The comparison was performed only for these two stations since they were the only ones coincident with the data available in Oliveira *et al.* [2006a].

At station L (Cais do Bico), the amplitude errors found in the present work are higher than the ones obtained by Oliveira *et al.* [2006a]. Indeed, in the present work, an amplitude error of about 36% was found for the main semidiurnal tidal constituent in this station. At station F (Costa Nova) the amplitude errors obtained for the new bathymetry were smaller for all the harmonic constituents represented, which means that the improvement of the horizontal grid leads to a better reproduction of the lagoon hydrodynamics near this station. Therefore, this comparison was not conclusive, and results for other stations should be compared.

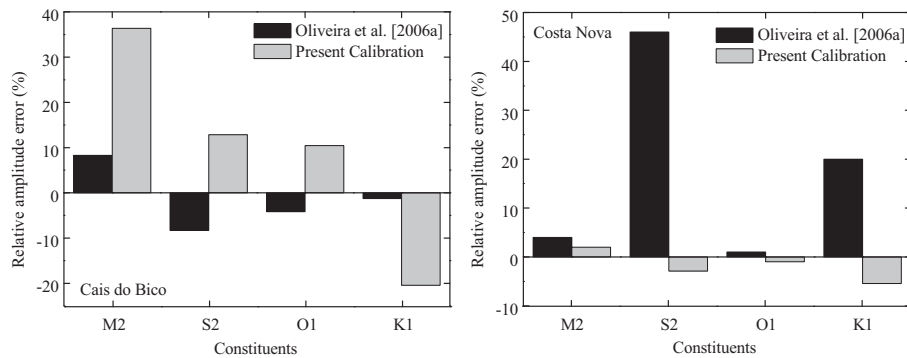


Figure 3.7: Comparison between the relative amplitude errors obtained in this work and obtained by Oliveira *et al.* [2006a], for two stations (Cais do Bico and Costa Nova) of the Ria de Aveiro.

Although studies for other areas revealed that the harmonic constants may be not really independent of time [Smith, 1997], several authors in their numerical modelling calibration studies consider the harmonic constants as invariants characteristics of the astronomic tide at a specific site [Cheng *et al.*, 1993; Martins *et al.*, 2002]. A long term analysis of the harmonic constants at Ria de Aveiro inlet revealed that the meaningful changes are only observed at a large temporal scale [Tomás and Dias, 2004].

Because in this case the model results and data are also compared based on frequency domain properties, there is no time distinction between model calibration and model validation [Cheng *et al.*, 1993]. Thus, in the present work it was decided that model validation was not necessary and the harmonic constants were considered independent of time.

Since the stations I, J and K are relevant for the present work, because they are located in the central zone of the Ria de Aveiro (where the salt pans are located), and there are available data of current velocity for these stations, a comparison between model results and observed current velocity was also performed and is presented in Figures 3.8, 3.9 and 3.10.

When comparing current velocity values it is important to remember that this variable varies rapidly in space, both in magnitude and direction, from point to point. This behaviour reflects the irregular geometry of the region and it produces higher discrepancies between field and computed results.

For all three stations the model represents well the phase of the water velocity, but reveals some differences in its intensity (Figures 3.8, 3.9 and 3.10). The differences may be due to several factors such as bathymetric inaccuracies and the fact that the model results represent the mean value over the vertical, while the field data corresponds to an average over three points (surface, middle water and bottom).

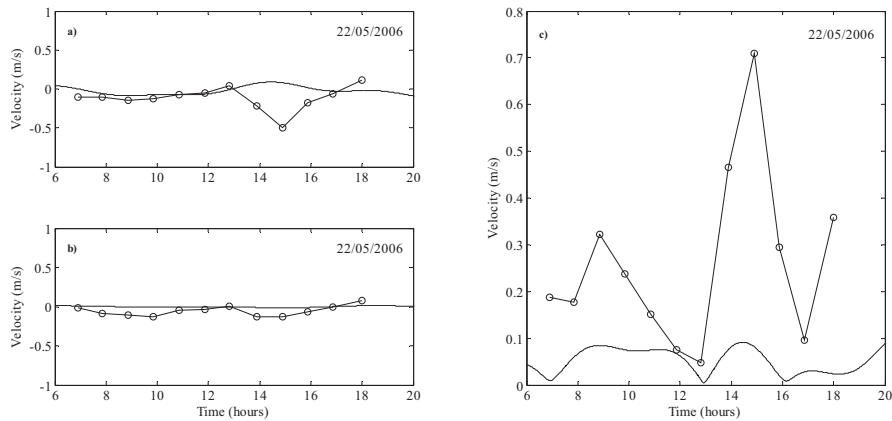


Figure 3.8: Times series of current velocity at station I: a) zonal component; b) meridional component; c) intensity (solid line: model results; circles: measurements).

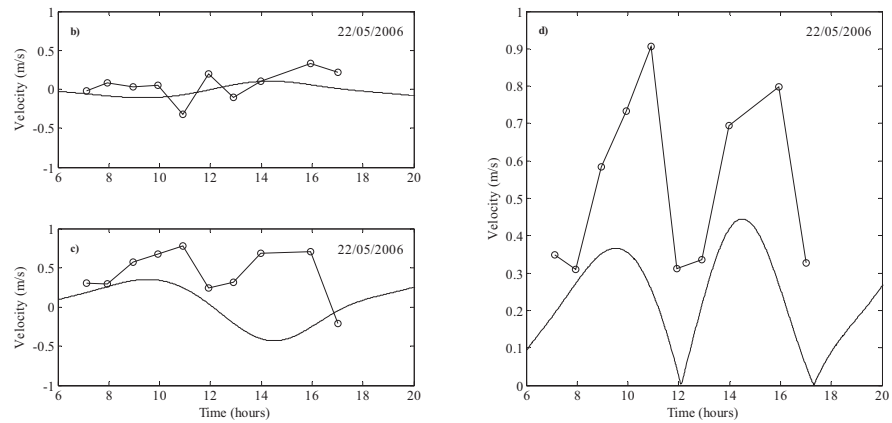


Figure 3.9: Times series of current velocity at station J: a) zonal component; b) meridional component; c) intensity (solid line: model results; circles: measurements).

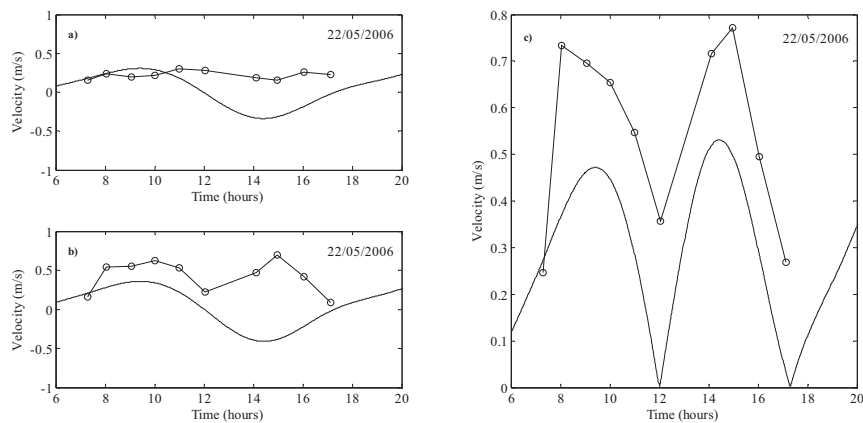


Figure 3.10: Times series of current velocity at station K: a) zonal component; b) meridional component; c) intensity (solid line: model results; circles: measurements).

Moreover, the model was only forced by tides, neglecting the wind and freshwater inflow influence. This factor may also contribute to the differences found in the water velocity time series

for these stations. Another factor that may contribute to these discrepancies is that measurements were performed every hour. This factor together with the velocity rapid variations did not allow an accurate description of the current speed, omitting some important information. For example, at station J (Figure 3.9 c)) between 12 and 13 hours there is no information of the tidal current in the measurements, and therefore the tidal inversion is not contemplated.

At station I the strong currents found in measurements could be explained by the fact that near this station exists a degraded salt pan wall. The salt pan is transformed in a water reservoir during the flood and then, the ebb originates high currents to the adjacent channel and model cannot reproduce it. For example, at 15 hours, which corresponds to the ebb, the difference between model and data is about 0.6 m/s. These strong ebb currents could provoke the faster degradation of the walls of the neighbour salt pans.

In general, it can be considered that model can reproduce the current velocity for these stations however differences between model and field data exist. These differences are due to several factors, such as an inaccurate definition of the bathymetry, very narrow channels that are not well resolved by the horizontal grid and some uncertainties in the field data.

4. Hydrodynamic changes induced by salt pans walls degradation

As referred in previous chapters a large area of salt pans in Ria de Aveiro reveals a high level of degradation. Due to the large extension of this area, it is impossible to perform a study that covers all the salt field of Aveiro. Therefore, in this work a set of salt pans was defined in order to simulate the destruction of their protective walls and consequent flooding. The selection of the set of salt pans was based on two sources: the final report of INTERREG III B [2008] project, where a detailed characterization of the present situation of the salt pans walls is presented, and in satellite images of Google Earth that allow the identification of the degraded walls. This characterization reveals that the salt pans located in the Grupo do Mar and south of the Grupo do Norte are the most vulnerable to the strong currents.

Thus, from the present bathymetry, distinct grids were generated representing a sequential inundation of the Ria de Aveiro central area (Figure 4.1). The inundation was performed through the partial collapse of the salt pans walls, whose dimensions are in accordance with the ones presented in the final report of INTERREG III B [2008] project and with Google Earth images. The flooded area for each case study has a constant depth equal to 1 m, above to the mean sea level (2 m).

To achieve the final goal of this work, the model ELCIRC was run for the entire Ria de Aveiro for the present bathymetry and for the four case studies presented in Figure 4.1. Possible changes in overall and local hydrodynamic regime are evaluated in the next sections. This evaluation is performed through the analysis of tidal currents for A, B and C areas represented in Figure 4.1, the tidal asymmetry along the axis of the main channels of the lagoon and the tidal prism for several cross-sections along the lagoon, determined for each simulation.

The total area and volume of the entire lagoon above the mean sea level for the present bathymetry and for all the case studies are quantified in Table 4.1. In this table differences between each case study and the present bathymetry are also presented, in percentage. The total area and volume increase about 5.61% and 3.49%, respectively, from the present bathymetry to the case study 4.

Table 4.1: Total area and volume for each bathymetry and differences in percentage.

Grids	Area ($\text{m}^2 \times 10^6$)	Volume ($\text{m}^3 \times 10^6$)	% Δ Area	% Δ Volume
			Relative to the present bathymetry	
Present bathymetry	55.66	98.04	-	-
Case Study 1	56.56	99.07	1.62	1.05
Case Study 2	57.93	100.65	4.08	2.66
Case Study 3	58.42	101.10	4.96	3.11
Case Study 4	58.78	101.46	5.61	3.49

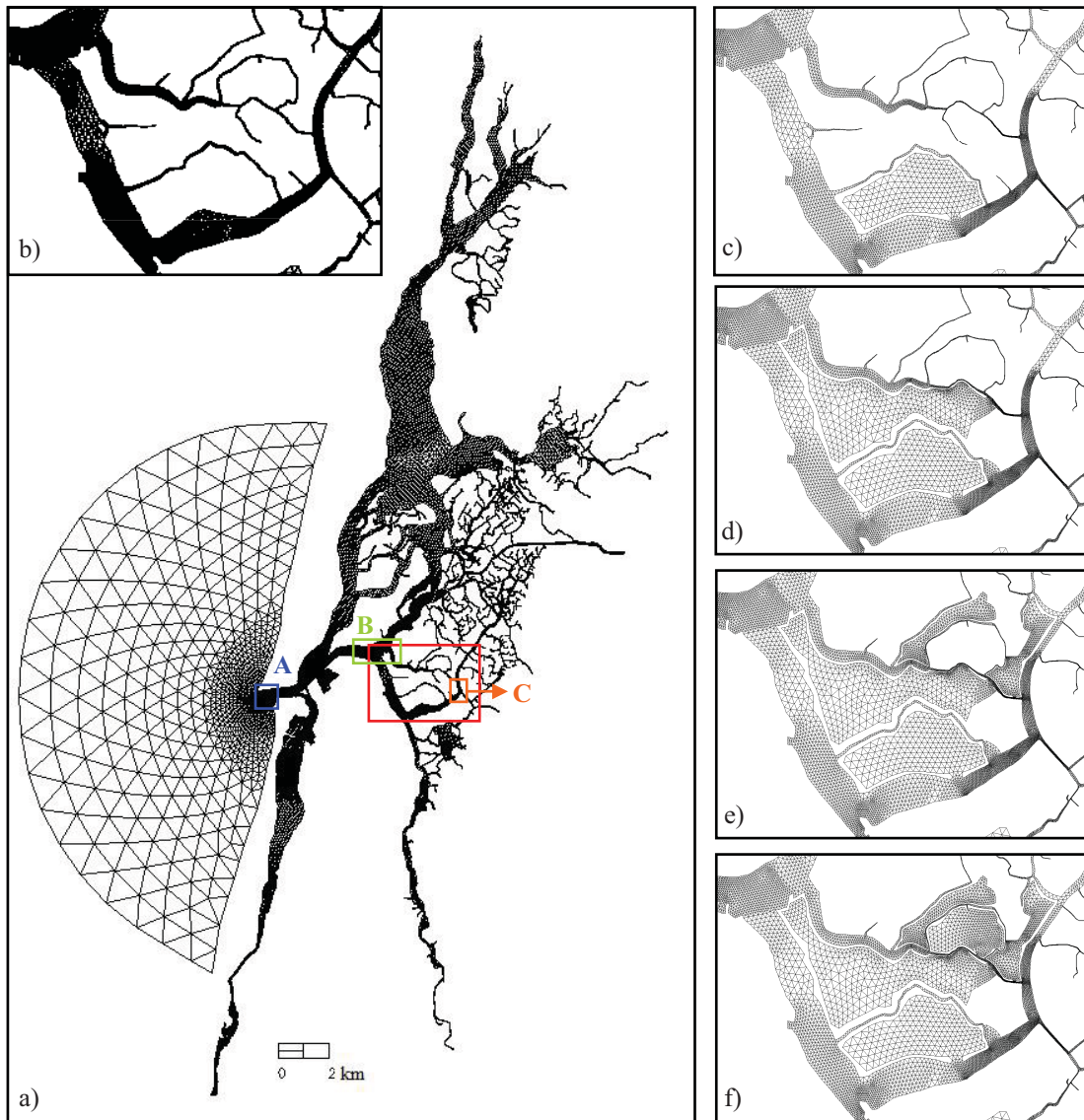


Figure 4.1: Horizontal grid of the Ria de Aveiro: a) Full grid with the red rectangle representing the study area. A, B and C are the selected areas where the velocities are represented; b) Detail of the grid in study area; c) Case Study 1; d) Case Study 2; e) Case Study 3; f) Case Study 4.

4.1 Tidal Currents

Several simulations for all the bathymetries represented in Figure 4.1 were performed in order to study the impact of salt pans walls destruction in the lagoon hydrodynamics, both in neap and spring tides. Due to the restrict space available in this manuscript, only simulations for the present bathymetry and for the case study 4 (only in spring tides) are presented.

In this section the response of the magnitude of flood and ebb velocities to bathymetric changes (increase of the lagoon total area) is evaluated. Thus, the velocities are only represented near the

inlet (A in Figure 4.1), near the station C (B in Figure 4.1) and near the station D (C in Figure 4.1). A, B and C were chosen due to its location, in the entrance of the lagoon, and upstream and downstream of the study area, respectively.

Figure 4.2 shows the magnitude of the flood and ebb velocities in spring tide near the inlet for the present bathymetry and for case study 4.

Generally, tidal current velocities in the present bathymetry are smaller than in the case study 4, throughout the tidal cycle. For both bathymetries the model results also show that current velocity is systematically larger on ebb than on flood, revealing ebb-dominance of the inlet.

According to model results, for spring tide condition, maximum ebb and flood velocities are 1.94 m/s and 1.85 m/s, respectively, for the present bathymetry and are 2.06 m/s and 1.96 m/s for the case study 4, which corresponds to an increase of about 6% for the ebb and about 5% for the flood. This increase of tidal currents corresponds to an increase of about 5.61% (Table 4.1) in the lagoon area. For neap tide condition, an increase of about 6% and 9% is observed in ebb and flood velocities near the lagoon mouth, respectively.

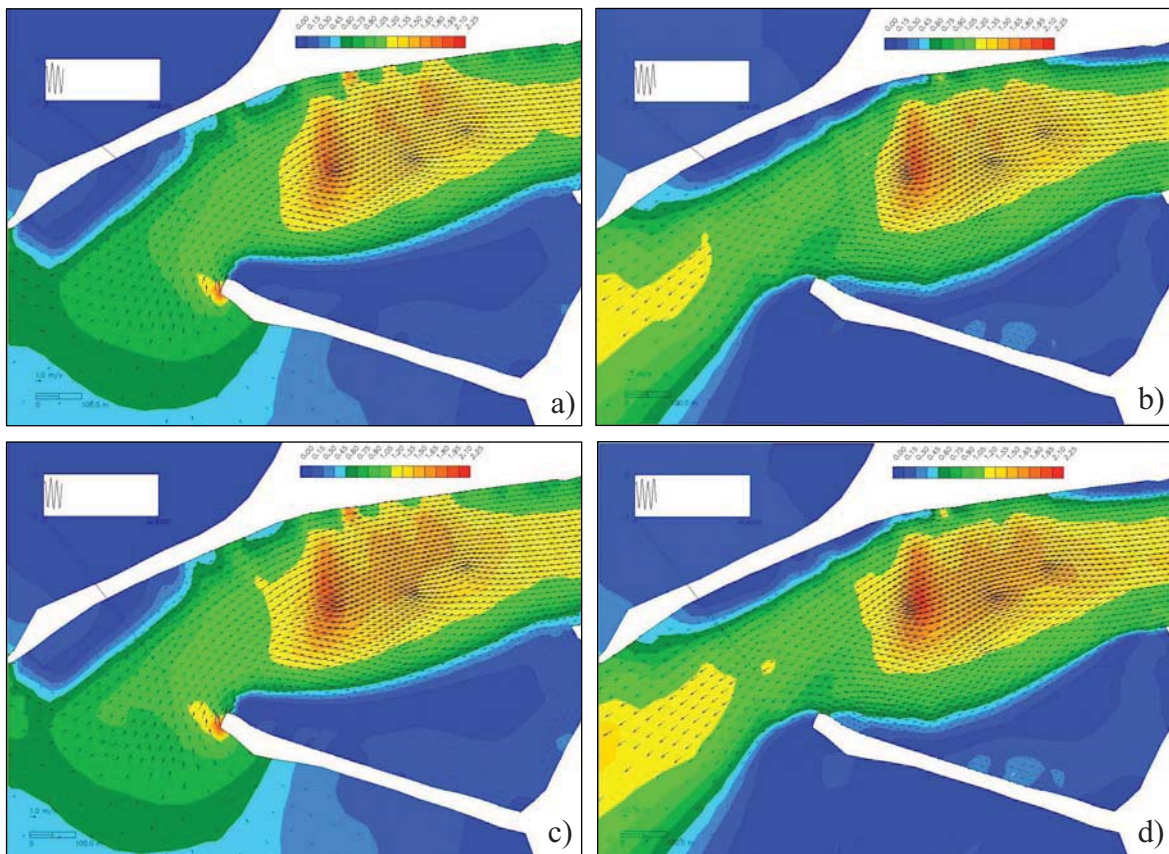


Figure 4.2: Magnitude of velocity in m/s during spring tide near the inlet of the lagoon (A in Figure 4.1). Above: a) Flood and b) ebb currents for the present bathymetry. Below: c) Flood and d) ebb currents for the case study 4.

This tendency was observed for all the cases study (not represented here), i.e. an increase in the total area of the lagoon increases the current velocity near the lagoon's mouth.

Model results also reveal a phase lag between tidal velocity and sea level elevation. For all the bathymetries, the maximum flood velocity is reached about 1.5 h before high tide and the maximum ebb velocity is reached about 3 h before low tide. Therefore, the maximum flood velocities occur at higher levels than the maximum ebb velocities, which also contribute to ebb-dominance in the lagoon mouth.

Figure 4.3 represents the magnitude of flood and ebb velocities for the present bathymetry and for the case study 4 near the station C (B in Figure 4.1).

In general, model results show that the current velocity increases with the expansion of the flooded area. For instance, in the beginning of the Ílhavo channel an increase of 5.61% in the total area of the lagoon leads to an increase of about 0.2 m/s in both ebb and flood currents.

The magnitude of ebb and flood currents on spring tide were also represented (Figure 4.4) near stations D, J and K (C in Figure 4.1). Model results show a significant increase of the tidal currents in this zone. The increase of tidal currents with the expansion of the lagoon area is observed for all the case studies (not represented).

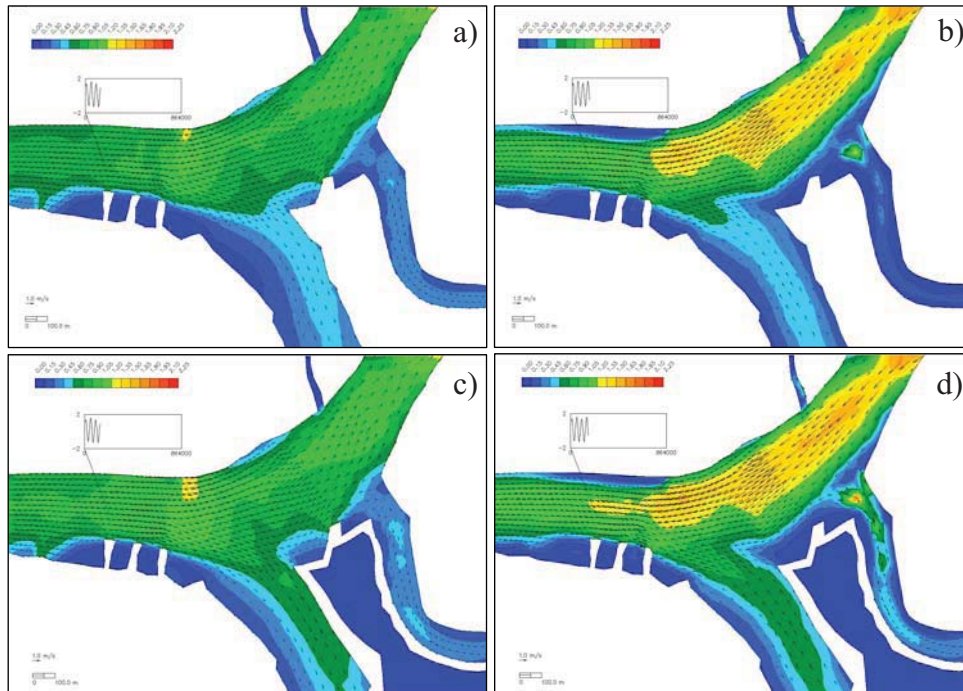


Figure 4.3: Magnitude of velocity in m/s during spring tide (B in Figure 4.1). Above: a) Flood and b) ebb currents for the present bathymetry. Below: c) Flood and d) ebb for the case study 4.

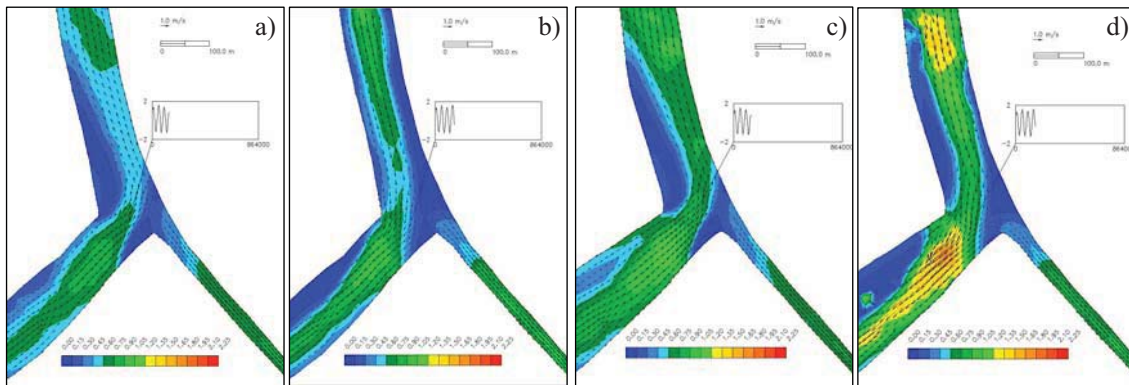


Figure 4.4: Magnitude of velocity in m/s during spring tide (C in Figure 4.1). Left: a) Flood and b) ebb currents for the present bathymetry. Right: c) Flood and d) ebb for the case study 4.

From the previous results it can be considered that the central area of the Ria de Aveiro lagoon presents ebb currents larger than flood ones, showing ebb-dominated channels. This fact is amplified with the increasing of the flooded area, due to the salt pans walls destruction, that induces higher velocities, mainly during the ebb and in the lagoon central area.

The maximum tidal currents are summarized in Table 4.2, for each case study and for the three studied areas. The maximum values are presented in this work as a parameter representing the velocity trend along the case studies.

According to the values presented in Table 4.2 the maximum values of tidal currents are systematically larger on ebb than on flood.

An increase of the maximum tidal currents is observed from the present bathymetry to the case study 4 for A, B and C areas. The largest changes in maximum tidal currents occur in neap tides and between cases study 1 and 2, which corresponds to an increase of 2.46% in the total lagoon area.

Near the lagoon mouth (A in Figure 4.1) and near station C (B in Figure 4.1) the increase of the maximum tidal currents is lower than 2% between the case studies 3 and 4. These results were expected since the differences in the lagoon area and volume are only 0.62% and 0.36%, respectively. Relatively to the area C there are significant differences between the results for case studies 3 and 4. For instance, in neap tide condition an increase of 30% was found during the flood.

In conclusion, the increasing of tidal currents with the lagoon area expansion is more significant as the distance from the inlet increases and in neap tide conditions.

Nevertheless, the results show clearly that an increase in the lagoon area will increase the tidal currents intensity along the main channels of the lagoon.

Table 4.2: Magnitude of the maximum velocity in m/s in areas A, B and C.

Area		Magnitude of velocity (m/s)			
		Neap Tide		Spring Tide	
		Max. Flood	Max. Ebb	Max. Flood	Max. Ebb
A	Present bathymetry	0.43	0.60	1.85	1.94
	Case Study 1	0.43	0.61	1.88	1.97
	Case Study 2	0.45	0.63	1.94	2.05
	Case Study 3	0.46	0.63	1.95	2.05
	Case Study 4	0.47	0.64	1.96	2.06
B	Present bathymetry	0.25	0.46	1.12	1.55
	Case Study 1	0.26	0.47	1.20	1.56
	Case Study 2	0.28	0.50	1.21	1.57
	Case Study 3	0.29	0.52	1.22	1.59
	Case Study 4	0.29	0.52	1.24	1.62
C	Present bathymetry	0.08	0.19	0.84	1.00
	Case Study 1	0.10	0.20	0.89	1.10
	Case Study 2	0.19	0.45	1.00	1.40
	Case Study 3	0.20	0.48	1.15	1.55
	Case Study 4	0.26	0.67	1.22	1.65

4.2 Tidal Asymmetry

The information about tidal asymmetry can be a useful tool to evaluate the flow pattern in shallow estuaries and to characterize the dominance of flood or ebb flow [Sivakholundu *et al.*, 2006].

Although oceanic tides typically exhibit ebbs and floods with similar durations, the deformation of tides in shallow waters usually leads to significant differences between these durations [Aubrey and Speer, 1985]. When the tide rises faster than it falls, velocities tend to be higher on flood than on ebb because of continuity. Along much of the world's coastlines as well as in Ria de Aveiro, the dominant astronomical constituent is M_2 , the semi-diurnal lunar tide. Because of M_2 dominance, the most significant overtide formed in these well mixed estuaries is M_4 , the first harmonic of M_2 [Friedrichs and Aubrey, 1988]. The M_4 constituent is generated primarily through non-linear interactions in the equation of motion and continuity, but friction can also play a minor role [Parker, 1991]. In Ria de Aveiro lagoon, the amplitude of the M_4 constituent increases from the lagoon mouth toward the end of channels. The most important consequence of this growth is the differentiation of the ebb and flood durations, leading to an asymmetric propagation of the tide.

A direct measurement of non-linear distortion, the M_4 to M_2 sea-surface amplitude ratio is defined as $A_r = A_{M_4} / A_{M_2}$ and indicates the magnitude of the tidal asymmetry generated within the estuary. An undistorted tide has an amplitude ratio of zero. The larger A_r , more distorted is the tide

and more strongly flood or ebb dominant the system becomes. The sea-surface phase of M_4 relative to M_2 is defined as $\varphi = 2\theta_{M_2} - \theta_{M_4}$ and determines the orientation of tidal distortion ($0^\circ < \varphi < 180^\circ$ indicates flood dominance and $180^\circ < \varphi < 360^\circ$ indicates ebb dominance).

The amplitude and the phase of M_2 and M_4 tidal constituents were determined for the Ria de Aveiro using model results, for the present bathymetry and for all the case studies. However due to the lack of space in this work, only the results for the present bathymetry and for the case study 4 are presented (Figures 4.5 and 4.6, respectively).

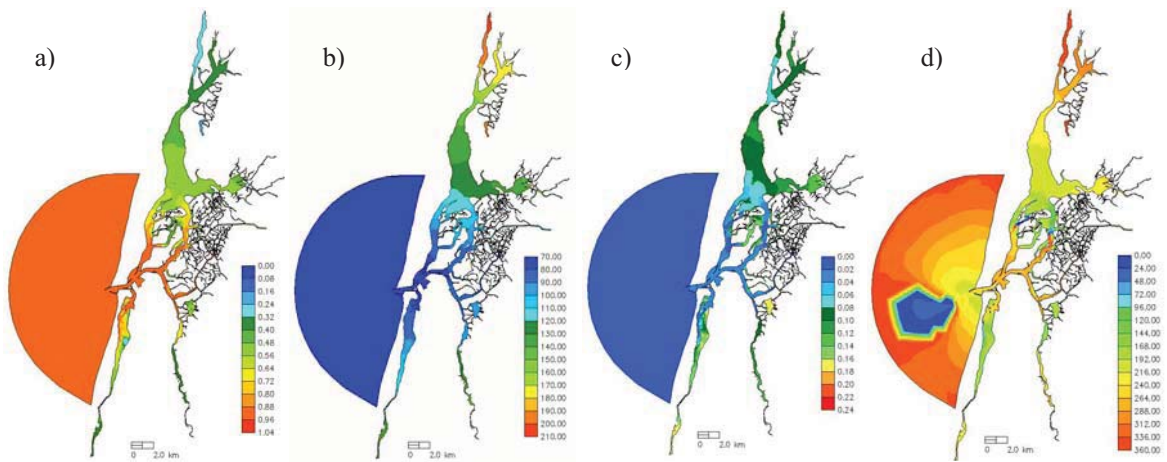


Figure 4.5: Present bathymetry: a) Amplitude (m) distributions for the M_2 constituent; b) Phase ($^\circ$) distributions for the M_2 constituent; c) Amplitude (m) distributions for the M_4 constituent; d) Phase ($^\circ$) distributions for the M_4 constituent.

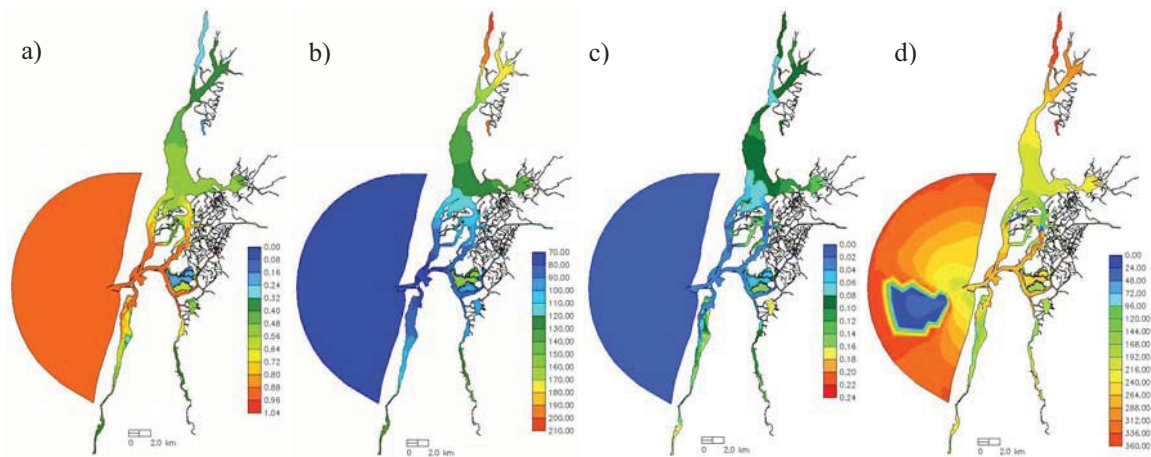


Figure 4.6: Case Study 4: a) Amplitude (m) distributions for the M_2 constituent; b) Phase ($^\circ$) distributions for the M_2 constituent; c) Amplitude (m) distributions for the M_4 constituent; d) Phase ($^\circ$) distributions for the M_4 constituent.

The M_2 constituent has most of the tidal energy in Ria de Aveiro [Dias, 1999; Vaz *et al.*, 2007b], and for that reason can be considered representative of the tide in this lagoon. The tides propagate into the lagoon and are altered by the channels geometry and bathymetry. The amplitudes are almost constant in the lagoon central area, and rapidly decrease toward the end of channels, where their values are very low. This pattern is in accordance with previous results of Dias *et al* [2000]. For instance, model results for the present bathymetry reveal that the amplitude of the M_2 constituent near the lagoon's mouth is about 0.94 m and at the far end of S. Jacinto channel is about 0.62 m, which reveals a decrease of about 36.7%.

For the present bathymetry, results also reveal that there are rapid phase changes as the tide propagates to the North through the S. Jacinto and Espinheiro channels, and at their far end the phase delay is around 151° (~5 hours). This result is higher than the one computed by Dias *et al.* [2000], that observed a phase lag of about 130° .

Araújo *et al.* [2008] analysed possible responses of the Ria de Aveiro to changes in the lagoon area. They concluded that an increase in the total area of the lagoon decreases the amplitude and increases the tidal phase inside the lagoon. In fact, increasing the lagoon total area, due to the salt pans walls collapse, will generally lead to a decrease in the amplitude and an increase in the phase of M_2 and M_4 constituents (Figures 4.5 and 4.6). For instance, near the lagoon mouth, an increase of 5.61% in the lagoon flooded area (case study 4 to present bathymetry pattern) results in a decrease of 1% and 4% of the M_2 and M_4 amplitude, respectively.

An interesting feature occurs in the flooded area. Amplitudes of the M_2 constituent range between 0.56 and 0.64 m in the flooded area corresponding to the case study 1, nevertheless of the corresponding area to the other case studies, the amplitude is extremely reduced (minimum value of 0.08). The same pattern can be observed for M_4 amplitude.

In summary, an increase of the lagoon total area leads to a decrease in the amplitude and an increase in the phase of the major tidal constituent, M_2 , along the Ria de Aveiro, as well as in their first harmonic, M_4 , in accordance with the previous results of Araújo *et al.* [2008].

The amplitude ratio, the relative phase and the difference between ebb and flood durations were computed along the axis of the four main channels of the Ria de Aveiro and for all the case studies (Figure 4.7), in order to evaluate the tidal asymmetry, as well as the response of these parameters to an increase in the lagoon total area. Because tidal levels exhibit very small variations across the channels, all these parameters were computed along the channels axis. For the ebb-flood differences, the negative values indicate ebb duration lower than flood one (ebb currents are higher than flood currents), which leads to ebb dominance and positive values indicate flood dominance.

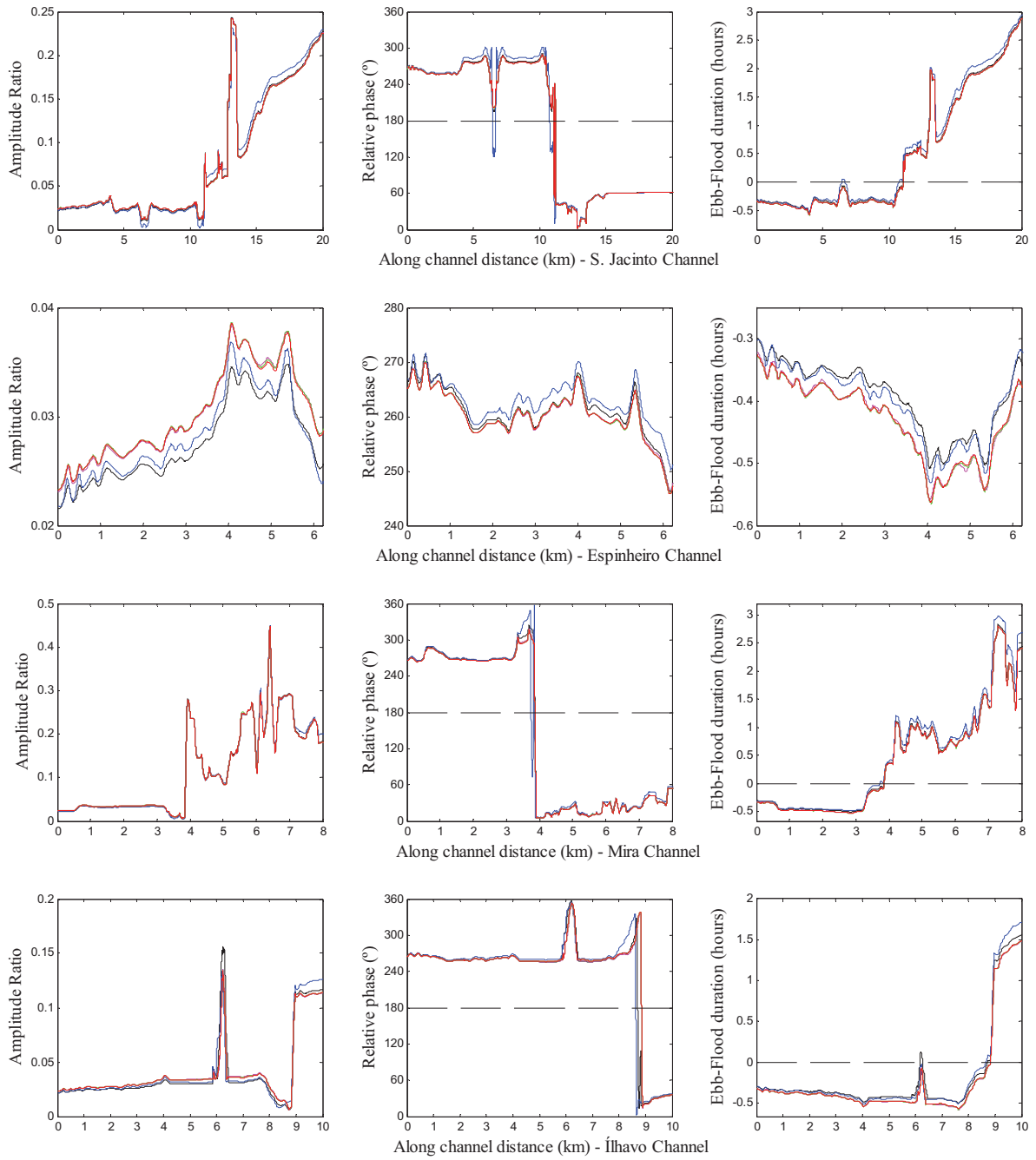


Figure 4.7: Asymmetric coefficients: Amplitude Ratio, Relative Phase (°) and difference between ebb and flood duration (hours) along the axis of the four main channels of the Ria de Aveiro. (— Present Bathymetry, — Case Study 1, — Case Study 2, — Case Study 3 and — Case Study 4).

Generally, the tidal asymmetry increases from the lagoon mouth toward the upper reaches of the lagoon. In fact, near the lagoon mouth A_r is very small (close to 0), increasing to values close to 0.4 toward the far end of the lagoon.

According to the model results there are both ebb and flood dominated areas in Ria de Aveiro, in accordance with the results presented by Dias [2001] and Oliveira *et al.* [2006a]. This trend is observed for all the cases study presented. However, the tidal asymmetry becomes strongest, when increasing the lagoon total area. Indeed, the amplitude ratio increases with the lagoon's area increase. For instance, near the lagoon mouth, an increase of 5.61% of the lagoon total area slight increases the amplitude ratio (about 8%). Comparing the ebb-flood difference for all the case studies, it was concluded that, near the lagoon mouth, this difference becomes more negative with the increase of the lagoon area, which leads to a strongest ebb dominance.

Generally the main differences were observed along the S. Jacinto and Espinheiro channels. Along the S. Jacinto channel there are both ebb and flood dominated areas. Until 13 km away from the lagoon mouth this channel is ebb dominated and from this distance to the end, becomes flood dominated. According to the model results when the lagoon area is increased, the amplitude ratio, regarded as a measured of tidal asymmetry, increases in the first half of the channel and slightly decreases from this distance toward the upper channel. Hence, this channel becomes more ebb dominated in the first half and less flood dominated in the upper reaches of the channel.

The relative phase of M_4 with respect to M_2 in Espinheiro channel shows a slight decrease with the expansion of lagoon total area, indicating that the characteristics of the tidal asymmetry are changing along this channel. In fact, the increase of the lagoon total area results in the decrease of ebb-flood differences along the Espinheiro channel, which means that this channel becomes more ebb dominated.

According to the model results, along the Mira channel differences between the present bathymetry and the case studies are almost null, which means that the flooded area is located in a zone that may not affect the tidal asymmetry pattern in this channel.

At the beginning of Ílhavo channel (~6 km away from the lagoon mouth) ebb-flood differences decrease around 12% with the lagoon total area expansion of 5.61%.

In conclusion, the tidal asymmetry patterns were the same for all the cases, i.e. the central zone remains ebb-dominant and the upper lagoon flood-dominant when increasing the lagoon area. An increase of the lagoon total area leads to an increase in tidal asymmetry, mainly in the S. Jacinto and Espinheiro channels.

Furthermore, if the amplitude and phase of the major tidal constituent and its first harmonic changes with the increase of the lagoon total area, thus tidal asymmetry should also be altered.

The results of ebb and flood currents obtained in the previous section, corroborate the increase of the ebb dominance in the lagoon central area.

4.3 Tidal Prism

The tidal prism may be determined for several cross-sections of the lagoon using the numerical model results. In this study, the tidal prism is defined as the volumetric flux passing a cross-section in a flooding cycle. Clearly, the tidal prism is not only a function of the location of the cross-section, but also a function of the tides (spring-neap). The tidal prism was computed for fifteen cross-sections in the central area of the Ria de Aveiro lagoon as shown in Figure 4.8, for all the case studies. Simulations were performed for extreme spring and neap tides (~ 3 m and ~ 0.7 m of amplitude, respectively), as well as for an average tide case (~ 1.2 m of amplitude).

Figure 4.9 represents the tidal prism determined for the fifteen cross-sections. For all the case studies the highest values of tidal prism are found in spring tide, and the lowest in neap tide, reinforcing the importance of the fortnight modulation in the Ria de Aveiro.

Largest values of tidal prism are found near the lagoon mouth (section number 1 in Figure 4.8) and decrease with the distances of the cross-sections to the lagoon entrance. At the cross-section close to the lagoon mouth the estimated tidal prism is about $86.30 \times 10^6 \text{ m}^3$ for a maximum spring tide, lower than the computed by Dias [2001], and $30.99 \times 10^6 \text{ m}^3$ for a minimum neap tide, for the present bathymetry. According to the results presented in Figure 4.9 the tidal prism for each one of the main channels relative to its value at the mouth of the lagoon is about 44% for S. Jacinto channel, 25% for Espinheiro channel, 11% for Mira channel and 12% for Ílhavo channel. Comparing to those given by Dias [2001] the values of tidal prism are higher for the S. Jacinto channel ($\sim 9\%$) Espinheiro ($\sim 0.6\%$) and Mira ($\sim 1\%$) channels, and are lower for the Ílhavo ($\sim 1.5\%$) channel.

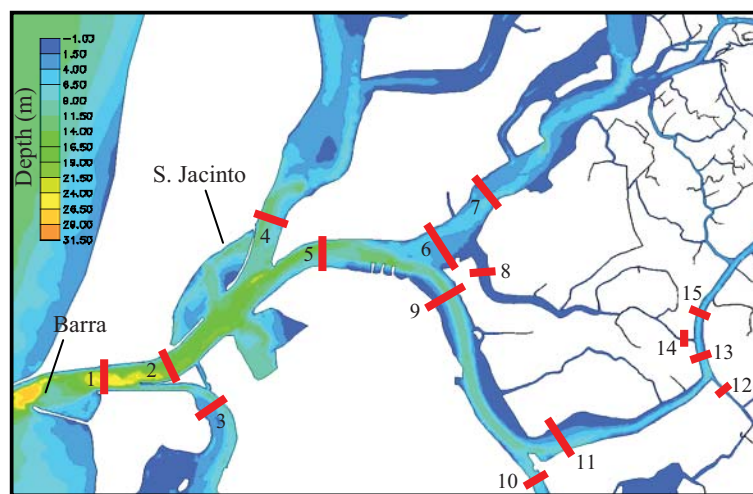


Figure 4.8: Cross-sections location, where the tidal prism were computed.

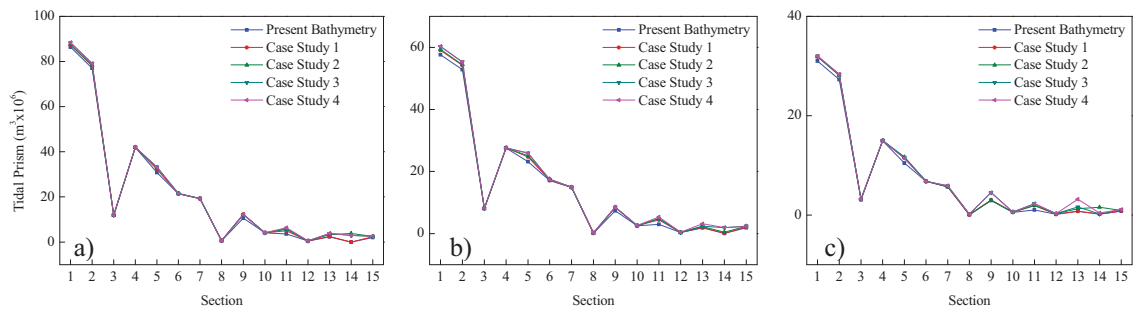


Figure 4.9: Computed tidal prism at 15 cross-sections of the Ria de Aveiro, at a) maximum spring tide, b) mean tide and c) minimum neap tide for the present bathymetry and for each case study.

The increase of the lagoon volume, resulting from the larger number of salt pans with their walls destroyed, increase the tidal prism in the Ria de Aveiro lagoon, as shown in Figures 4.9 and in Table 4.3.

According to the model results presented in Table 4.3, an increase of 5.61% in the lagoon total area leads to an increase of 2.33% for the maximum spring tide, for the tidal prism at the inlet. For the average tide the tidal prism increases 4.62%, and 3.21% for the neap tide condition.

The highest increase of the tidal prism was found near the flooded area. Indeed, at cross-section 14 the tidal prism strongly increases with the expansion of the lagoon total area. For instance, in neap tide condition an increase of about 150% was observed. The strong increase of tidal prism in this cross-section is induced by the large increase of the lagoon area near the cross-section 14, due the salt pans walls collapse around that channel.

Table 4.3: Tidal prism for all the cross-sections for the present bathymetry and relative differences for each case study and present bathymetry.

Cross-Section	Tidal Prism (m ³ x10 ⁶)			Tidal Prism %Δ (relative to the present bathymetry)											
	Present bathymetry			Neap Tide				Mean Tide				Spring Tide			
	Neap Tide	Mean Tide	Spring Tide	Case Study1	Case Study2	Case Study3	Case Study4	Case Study1	Case Study2	Case Study3	Case Study4	Case Study1	Case Study2	Case Study3	Case Study4
1	31.00	57.64	86.34	2.77	2.80	3.38	3.21	2.49	3.00	4.61	4.62	1.11	1.46	2.30	2.33
2	27.27	52.81	77.00	3.17	3.18	3.85	3.88	2.67	2.99	4.76	4.59	1.30	1.69	2.73	2.71
3	3.07	8.07	11.84	2.86	3.95	4.43	4.34	0.66	0.61	0.63	0.92	0.02	0.04	0.42	0.44
4	14.92	27.59	41.88	0.35	0.47	0.48	0.42	0.02	0.03	0.04	0.13	0.01	0.26	0.28	0.29
5	10.43	23.14	30.80	10.02	11.83	11.52	9.23	6.91	8.22	12.11	11.87	4.55	6.82	7.84	7.67
6	6.76	17.10	21.35	0.08	0.69	0.10	0.04	0.58	2.65	1.95	1.92	0.04	0.69	0.90	0.68
7	5.70	14.88	19.24	0.01	0.03	2.78	2.90	0.09	0.12	0.48	0.52	0.11	0.22	0.11	0.01
8	0.04	0.13	0.56	17.87	75.43	329.53	327.22	0.12	19.30	107.40	108.93	2.70	3.45	18.05	19.30
9	2.92	7.39	10.60	2.51	2.21	54.00	54.45	15.05	14.51	14.55	14.63	15.09	15.19	15.25	15.59
10	0.53	2.53	4.08	5.22	13.23	13.42	13.59	1.46	1.49	1.83	2.42	0.10	0.16	0.09	0.02
11	0.99	2.99	3.58	89.04	95.53	130.63	131.10	47.75	62.03	60.60	78.95	39.11	55.87	69.37	77.24
12	0.14	0.35	0.44	3.73	75.65	69.91	74.42	6.43	14.83	14.74	23.04	1.81	9.95	10.18	10.26
13	0.75	1.89	2.30	0.20	69.94	116.15	322.66	0.05	18.71	28.10	67.77	4.35	43.04	64.22	68.83
14	0.16	0.10	0.02	9.63	899.42	23.51	150.94	1.47	409.19	1896.17	1937.64	0.77	15345.38	11656.95	11717.05
15	0.77	1.90	2.06	1.30	18.26	32.99	42.43	8.78	25.14	26.49	21.34	13.59	21.02	20.95	26.88

Generally, the increase of the lagoon total area, due to the salt pans walls collapse, results in an increase in the tidal prism, with the higher values at the cross-sections close to the flooded area.

5. Conclusion

The main aim of this work was to contribute to understand the consequences of the partial salt pans walls destruction on the entire Ria de Aveiro lagoon hydrodynamics. With this purpose, a finite volume shallow water model (ELCIRC) was implemented and calibrated for the Ria de Aveiro.

ELCIRC was previously implemented in the Ria de Aveiro by Oliveira *et al.* [2006a], in order to study its inlet dynamics in terms of tidal propagation, as well as to study the variability of tidal asymmetry in the upper and lower lagoon. In this study was developed a horizontal grid, which resolution was insufficient for the present work, since the narrow channels located in the lagoon central area were not represented. For that reason and taking into account the main aim of this work the existing grid was improved, adding and refining several channels, mainly in the lagoon central area, where salt pans are located.

Several model runs were performed to calibrate the model, adjusting the bottom stress in order to reduce the differences between the available data and model results. According to the final results, the model was considered successfully calibrated for a very complex system as Ria de Aveiro. Indeed, the RMS values range from 3% to 10% of the local amplitude and skill values higher than 0.95 were found for the most stations located in lagoon central area. However, differences between model and field data exist. These differences are due to several factors, such as very narrow lagoon channels that are not well resolved by the horizontal model grid, and some possible uncertainties in the field data, as well as due to possible inaccuracies in the bathymetry.

The M_4 constituent was not simulated with the expected accuracy. The errors found in the M_4 reproduction may be due to bathymetric errors that can not be corrected by the adjustment of the bottom coefficient. Moreover, according to Araújo *et al.* [2008] an average increase of 0.245 m in M_2 amplitude and an average 17.4° decrease in M_2 phase, over the 16 years were observed. As the bathymetric data and the water level field data used to calibrate the model were measured with the time gap of 16 years referred by Araújo *et al.* [2008] (bathymetric data was main collected in 1987/88 while the field data used in the M_4 calibration was collected in 2003) the errors in M_2 amplitude will induce errors in M_4 amplitude. Nevertheless, if M_2 amplitude changes of 0.245 m in 16 years, M_4 will also change, since the M_2 energy is almost all transferred to M_4 . However, as the M_4 constituent is generated through the non-linear interactions in the equations of motion and continuity, which are generally well adjusted by the model, the results for M_4 constituent are considered accurate enough to perform this study.

In order to evaluate the influence of the new bathymetry in the model's ability to reproduce the Ria de Aveiro lagoon hydrodynamics, the relative amplitude errors obtained in this work were compared with those obtained by Oliveira *et al.* [2006a]. Only two stations were compared (L and F) and was concluded that in the lagoon central area the relative amplitude errors obtained with the new bathymetry were smaller for all the constituents compared (M_2 , S_2 , K_1 and O_1), which means that the improvement of the horizontal grid leads to a better reproduction of the lagoon hydrodynamics.

Once calibrated, ELCIRC was used to characterize the Ria de Aveiro hydrodynamics under different scenarios: present bathymetry and projections of bathymetries resulting from the salt pans walls destruction and consequent increase of the flooding area in Ria de Aveiro.

In order to study the hydrodynamic responses of the Ria de Aveiro lagoon to bathymetric changes (the increasing of total lagoon area), tidal currents, tidal asymmetry and tidal prism were analysed for each case study. According to the model results, the ebb currents are larger than flood ones, showing ebb-dominated channels. This pattern is amplified with the increasing of the flooded area, which induces higher velocities, mainly in the lagoon central area during the ebb. Thus, the increase of tidal currents with the lagoon flooded area expansion is more significant as the distance from the inlet increases and with largest changes in neap tide condition.

Generally, the increase of the lagoon total area also results in an increase in the tidal prism, with the higher changes at the cross-sections close to the flooded area and in neap tide. In fact, the more significant increase of tidal currents and tidal prism in the lagoon central area is induced by the large increase of the lagoon flooded area near these channels.

The numerical results suggest that the response of the harmonic constants of the M_2 and M_4 constituents is affected by changes in the lagoon total flooded area. In fact, an increase in this area results in a decrease of their amplitudes and in an increase of their phases. Thereby, if the amplitude and phase of the major tidal constituent and its first harmonic changes with the increase of the lagoon flooded area, thus tidal asymmetry should also be altered. In fact, an increase of the lagoon flooded area leads to an increase in tidal asymmetry, mainly in the beginning of Ílhavo, in S. Jacinto and Espinheiro channels. Along the Mira channel the effect of the flooded area expansion in tidal asymmetry pattern is not significant. Thus, the tidal asymmetry pattern is mainly modified in the channels close to the flooded area.

In summary, an extreme destruction of the salt pans walls will result in a significant increase of the flooding area in the Ria de Aveiro, and therefore will affect the lagoon's hydrodynamic regime.

There are goals that remain for future. Namely, simulations including other areas that also reveal notorious degradation should be performed. Future work may also be conducted to address

the influence of the wind effect in the hydrodynamic regime. The improvement of the model calibration by using water level data acquired simultaneously with the bathymetric data should also be considered a future goal.

It is also important to use a numerical model to quantify the net sediment transport of cohesive sediment in the study area. The transport simulations will contribute to understand the bottom variations observed in the study area under the collapse of salt pans walls condition.

6. References

- Abecasis, C. K., 1961. As Formações Lagunares e seus Problemas de Engenharia Litoral (contribuição para um estudo sistemático). Instituto Superior Técnico, Lisboa.
- Abrantes, I., Dias, J. M., Rocha, F., 2006. Spatial and temporal variability of suspended sediments concentration in Ria de Aveiro Lagoon and fluxes between the lagoon and the ocean. *Journal of Coastal Research*, SI 39 (Proceedings of the 8th International Coastal Symposium), 718-723. Itajaí, SC, Brazil, ISSN 0749-0208.
- Almeida, M.A., Cunha, M., Alcantâra, F., 2001. Factors influencing bacterial production in a shallow estuarine system. *Microbial Ecology* 42 (3), 416-426.
- Araújo, I. G. B., 2005. Sea level Variability: Examples From the Atlantic Coast of Europe. Phd Thesis, School of the National Oceanography Centre, Southampton, UK.
- Araújo, I. B., Dias, J. M., Pugh, D. T., 2008. Model Simulations of tidal changes in a coastal lagoon, the Ria de Aveiro (Portugal). *Continental Research* 28, 1010-1025.
- Aubrey, D. G., Speer, P. E., 1985. A study of non-linear tidal propagation in shallow inlet/estuarine systems. Part I: Observations. *Estuarine, Coastal and Shelf Science* 21, 185-205.
- Baptista, A. M., Zhang, Y., Chawla, A., Meyers, E., Zulauf, M., 2004. A cross-scale model for 3D baroclinic circulation in estuary-plume shelf systems: II Application to the Columbia River. *Continental Shelf Research*.
- Barnes, R. S. K. (Ed.), 1980. Coastal lagoons. Cambridge: Cambridge University Press. 106 pp.
- Battaglia, B. (ed.), 1959. *Final resolution of the symposium on the classification of brackish waters*. *Archo Oceanography Limnology* 11 (suppl.): 243-248.
- Bellan, G. (ed.), 1987. *Ecologie Littorale Méditerranéenne*. Bulletin d'Ecologie 18, 106 pp.
- Burchard, H., Bolding, K., 2002. GETM, a general estuarine transport model: scientific documentation, tech. report, European Community, Ispra, Italy.
- Burchard, H., Bolding, K., Villarreal, M. R., 2004. Three-dimensional modelling of estuarine turbidity maxima in a tidal estuary. *Ocean Dynamics* 54, 250-265.
- Carrada, G. C., Cicogna, F., Fresi, E. (eds.) 1988. *Le lagune costiere: ricerche e gestione*. CLEM, Massa Lubrense, Napoli, Italy.

- Casulli, V., Cattani, E., 1994. Stability, accuracy and efficiency of a semi-implicit method for 3D shallow water flow, *Computers & Mathematics with Applications* 27, 99-112.
- Cheng, R. T., Burau, J. R., Gartner, J. W., 1991. Interfacing data analysis and numerical modelling for tidal hydrodynamic phenomena. In: Parker, B. B. E. (Ed.), *Tidal Hydrodynamics*. John Wiley and Sons, New York, USA, pp. 210-219.
- Cheng, R., T., Casulli, V., Gartner, J. W., 1993. Tidal, residual, intertidal mudflat (TRIM) model and its applications to San Francisco Bay, California. *Estuarine, Coastal and Shelf Science* 36, 235-280.
- Cunha, M. A., Almeida M., AlcantáraF., 2001. Short-time responses of the natural planktonic bacterial community to the changing water properties in an estuarine environment: ectoenzymatic activity, glucose incorporation and biomass production. *Microbial Ecology* 42 (1), 1-12.
- da Silva, J. F., Duck, R. W., 2001. Historical changes of bottom topography and tidal amplitude in Ria de Aveiro, Portugal – trends for future evolution. *Climate Research* 18, 17-24.
- Dias, J. M., 2001. Contribution to the study of Ria de Aveiro hydrodynamics. Ph. D. Thesis, University of Aveiro, Portugal, 288 pp.
- Dias, J. M., Fernandes, E. H., 2006. Tidal and subtidal propagation in two Atlantic estuaries: Patos lagoon (Brazil) and Ria de Aveiro Lagoon (Portugal). *Journal of Coastal Research*, SI 39 (Proceedings of the 8th International Coastal Symposium), 1422-1426. Itajaí, SC, Brazil, ISSN 0749-0208.
- Dias, J. M., Lopes, J. F., 2006a. Calibration and validation of hydrodynamic, salt and heat transport models for Ria de Aveiro lagoon (Portugal). *Journal of Coastal Research* SI 39, 1680-1684.
- Dias, J. M., Lopes, J. F., 2006b. Implementation and assesment of hydrodynamic, salt and heat transport models: the case of Ria de Aveiro Lagoon. *Environmental Modeling and Software* 21, 1-15.
- Dias, J. M., Lopes, J. F., Dekeyser, I., 1999. Hidrological characterization of Ria de Aveiro, Portugal, in early summer. *Oceanologica Acta* 22 (5), 473-485.
- Dias, J. M., Lopes, J. F., Dekeyser, I., 2000. Tidal propagation in Ria de Aveiro lagoon, Portugal. *Phys Chem Earth (B)* 25, 369-374.
- Dias, J. M., Lopes, J. F., Dekeyser, I., 2001. Lagrangian Transport of particles in Ria de Aveiro lagoon, Portugal. *Phys Chem Earth (B)* 26 (9), 721-727.

- Dias, J. M., Lopes, J. F., Dekeyser, I., 2003. A numerical system to study the transport properties in the Ria de Aveiro lagoon. *Ocean Dynamics* 53, 220-2231.
- Dias, J. M., Sousa, M. C., Bertin, X., Fortunato, A. B., Oliveira, A., 2009. Numerical modeling of the impact of the Ancão Inlet relocation (Ria Formosa, Portugal). *Environ. Model. Softw.* (2009), doi:10.1016/j.envsoft.2008.10.017, *in press*.
- Fortunato, A. B., Pinto, L., Oliveira, A., Ferreira, J. S., 2002. Tidally generated shelf waves off the western Iberian coast. *Continental Shelf Research* 22, 1935- 1950.
- Friedrichs, C. T., Aubrey, D. G., 1988. Non-linear tidal distortion in shallow well-mixed estuaries: a synthesis, *Estuarine, Coastal Shelf Science* 27, 521-545.
- Fry, V., Aubrey, D. G., 1990. Tidal velocity asymmetries and bedload transport in shallow embayments. *Estuarine, Coastal and Shelf Science* 30, 453-473.
- Guelorget O., Perthuisot J. P., 1983. Le dominance paraliq. Travaux du Laboratoire de Geologie Presses de l'Ecole Normale Superieure, Paris.
- Haidvogel, D. B., Arango, H. G., Hedstrom, K., Beckmann, A., Malanotte-Rizzoli, P., Shchepetkin, A. F., 2000. Model evaluation experiments in the North Atlantic Basin: Simulations in non-linear terrain following coordinates. *Dyn. Atmos. Oceans* 32, 239-281.
- Hsu, M. H., Kuo, A. Y., Kuo, J. T., Liu, W. C., 1999. Procedure to calibrate and verify numerical models of estuarine hydrodynamics. *Journal of Hydraulic Engineering*, 166-182.
- <http://earth.google.com/intl/pt/tour.html>www.google
- IH,1991. Instituto Hidrográfico. Recolha e processamento de dados de marés, correntes, temperaturas e salinidades na Ria de Aveiro. Tech. Rep. Relatório FT.MC. 5/87, Instituto Hidrográfico, Lisboa, Portugal.
- INTERREG III B, 2008. Projecto SAL – Sal do Atlântico. Acção6b – Protótipo de recuperação dos muros das marinhas, Relatório Final.
- Lasserre, P., Postma, H. (eds.), 1982. Proceedings of the internacional symposium on coastal lagoons, Bordeaux, France, 8-14 September 1981. *Oceanologica Acta*, special issue 461 pp.
- Li, M., Zhong, L., Boicourt, W. C., 2005. Simulations of Chesapeake Bay estuary: Sensitivity to turbulence mixing parameterizations and comparison with observations. *Journal of Geophysical Research* 110 (C12004), doi: 10.1029/2004JC002585.

- Lopes, J. F., Dias, J. M., Dekeyser, I. 2001. Influence of tides and river inputs on suspended sediment transport in the Ria de Aveiro lagoon, Portugal. *Phys. Chem Earth (B)* 26 (9), 729-734.
- Lopes, J. F., Dias, J. M., Dekeyser, I. 2006. Numerical modelling of cohesive sediments transport in the Ria de Aveiro lagoon, Portugal. *Journal of Hydrology* 319, 176-198.
- Martins, R. P., Vilela, C. P. X., Rosso, T. C. A., 2002. Hydrodynamic numerical modelling of Guanabara Bay, Rio de Janeiro, Brazil – A preliminar calibration. *Litoral* 2002, 329-335.
- Monismith, S. G., Fong, D. A., 1996. A Simple model of mixing in a stratified tidal flow. *Journal of Geophysical Research* 110, 28583-28595.
- Moreira, M. H., Queiroga, H., Machado, M. M., Cunha M. R., 1993. Environmental gradients in a southern estuarine system: Ria de Aveiro, Portugal, implication for a soft bottom macrofauna colonization. *Netherlands Journal of Aquatic Ecology* 27 (2-4), 465-482.
- Morgado, F., Queiroga, H., Melo, F., Sorbe, J. C., 2003. Zooplankton abundance in a coastal station of the Ria de Aveiro inlet (north-western Portugal): relations with tidal and day/night cycles. *Acta Oceanologica* 24, 175-181.
- Nunes Vaz, R. A., Lenon, G. W., de Silva Samarasinghe, J. R., 1989. The negative role of turbulence in estuarine mass transport. *Estuarine Coastal and Shelf Science* 28, 361-377.
- Nunes Vaz, R. A., Simpson, J. H., 1994. Turbulence closure modelling of estuarine stratification. *Journal of Geophysical Research* 99,16143-16160.
- Oliveira, A., Fortunato, A. B., Dias, J. M., 2006a. Numerical modelling of the Aveiro inlet dynamics. *Coastal Engineering*, 3282-3294.
- Oliveira, A., Fortunato, A. B., Pinto, L., 2006b. Modelling the hydrodynamics and the fate of passive and active organisms in the Guadiana Estuary. *Estuarine Coastal and Shelf Science* 70, 76-84.
- Oliveira, A., Fortunato, A. B., Rego, João R. L., 2006c. Effect of morphological changes on the hydrodynamics and flushing properties of the Óbidos lagoon (Portugal). *Continental Shelf Research* 26, 917-942.
- Parker, B. B., 1991. The relative importance of the various non-linear mechanisms in a wide range of tidal interactions. In: Parker B. B. (Ed.), *Tidal Hydrodynamics*. Wiley, New York, USA, pp. 237-268.

- Pawlowicz, R., Beardsley, B., Lentz, S., 2002. Classical tidal harmonic analysis including error estimates in MATLAB using T_TIDE. Canada. *Computers & Geosciences* 28, 929-937.
- Silva, J. F., 1994. Circulação da água na Ria de Aveiro – contribuição para o estudo da qualidade da água. Ph. D. Thesis, Universidade de Aveiro, Portugal, 158 pp.
- Simpson, J. H., Brown, J., Matthews, J., Allen, G., 1990. Tidal straining, density currents, and stirring in the control of estuarine stratification. *Estuaries* 13, 125-132.
- Sivakholundu, K. M., Kathioli, S., Mani, J. S., Idichandy, V. G., 2006. Evaluation of River Regulatory Measures in Hugly Estuary using Tidal Asymmetry Characteristics. *IEEE*.
- Stanev, E., Wolff, J. O., Burchard, H., Bolding, K., Floser, G., 2003. On the circulation in the East Frisian Wadden Sea: Numerical modelling and data analysis. *Ocean Dynamics* 53, 27-51.
- Smith, N. P., 1977. Meteorological and tidal exchange between Corpus-Christi Bay, Texas, and northwestern Gulf Mexico. *Estuarine Coastal Marine Science* 5, 511-520.
- Tomás, L. M., Dias, J. M., 2004. Tidal characterization at Ria de Aveiro inlet. In: *Littoral* 2004. 676-677 pp.
- Turner, P., Baptista, A. M., 1993. ACE/gredit User's Manual. Software for Semi-automatic Generation of Two-Dimensional Finite Element Grids. *Center for Coastal and Land-Margin Research, Oregon Graduate Institute of Science and Technology*.
- Vaz, N., Dias, J. M., Leitão, P., Martins, I., 2005. Horizontal patterns of water temperature and salinity in an estuarine tidal channel: Ria de Aveiro. *Ocean Dynamics* 55, 416-429.
- Vaz, N., Dias, J. M., Leitão, P. C., Nolasco, R., 2007b. Application of the Mohid-2D model to a mesotidal temperate coastal lagoon. *Computers & Geosciences* 33, 1204-1209.
- Vaz, N., Leitão, P. C., Dias, J. M., 2007a. Channel-ocean exchange driven by tides and river flow: Espinheiro Channel (Portugal). *Journal of Coastal Research*, SI 50 (Proceedings of the 9th International Coastal Symposium), 1000-1004. Gold Coast, Australia, ISSN 0749.0208.
- Warner, J. C., Geyer, W. R., Lerczak, J. A., 2005. Numerical modelling of an estuary: A comprehensive skill assessment. USA. *Journal of Geophysical Research* 110, C05001, doi: 10.1029/2004JC002691.
- Zhang, Y., Baptista, A., Meyers, E., 2004. A cross-scale model for 3D baroclinic circulation in estuary-plume-shelf systems: I. Formulation and skill assessment. *Continental Shelf Research* 24, 2187-2214.

- Zhong, L., Li, M., 2006. Tidal energy fluxes in the Chesapeake Bay. *Continental Shelf Research* 26, 752-770.